

# Xylem–phloem hydraulic coupling explains multiple osmoregulatory responses to salt stress

Saverio Perri<sup>1,2</sup> , Gabriel G. Katul<sup>3,4</sup>  and Annalisa Molini<sup>1,2</sup> 

<sup>1</sup>Masdar Institute, Khalifa University of Science and Technology, PO Box 54224, Abu Dhabi, United Arab Emirates; <sup>2</sup>Department of Civil Infrastructure and Environmental Engineering,

Khalifa University of Science and Technology, PO Box 127788, Abu Dhabi, United Arab Emirates; <sup>3</sup>Nicholas School of the Environment, Duke University, Durham, NC 27710, USA;

<sup>4</sup>Department of Civil and Environmental Engineering, Duke University, Durham, NC 27708, USA

Author for correspondence:

Saverio Perri

Tel: +971 (0)2 810 9231

Email: [saverio.perri@ku.ac.ae](mailto:saverio.perri@ku.ac.ae)

Received: 10 May 2019

Accepted: 11 July 2019

*New Phytologist* (2019) **224**: 644–662

doi: 10.1111/nph.16072

**Key words:** CO<sub>2</sub> enrichment, *halophytes*, osmoregulation, photosynthesis optimization, plant–water relations, salt tolerance, salt stress.

## Summary

- Salinity is known to affect plant productivity by limiting leaf-level carbon exchange, root water uptake, and carbohydrates transport in the phloem. However, the mechanisms through which plants respond to salt exposure by adjusting leaf gas exchange and xylem–phloem flow are still mostly unexplored.
- A physically based model coupling xylem, leaf, and phloem flows is here developed to explain different osmoregulation patterns across species. Hydraulic coupling is controlled by leaf water potential,  $\psi_l$ , and determined under four different maximization hypotheses: water uptake (1), carbon assimilation (2), sucrose transport (3), or (4) profit function – i.e. carbon gain minus hydraulic risk. All four hypotheses assume that finite transpiration occurs, providing a further constraint on  $\psi_l$ .
- With increasing salinity, the model captures different transpiration patterns observed in halophytes (nonmonotonic) and glycophytes (monotonically decreasing) by reproducing the species-specific strength of xylem–leaf–phloem coupling. Salt tolerance thus emerges as plant's capability of differentiating between salt- and drought-induced hydraulic risk, and to regulate internal flows and osmolytes accordingly.
- Results are shown to be consistent across optimization schemes (1–3) for both halophytes and glycophytes. In halophytes, however, profit-maximization (4) predicts systematically higher  $\psi_l$  than (1–3), pointing to the need of an updated definition of hydraulic cost for halophytes under saline conditions.

## Introduction

Over the last decades, soil salinization has grown at an unprecedented rate, becoming a global environmental issue (Datta & Jong, 2002; Schofield & Kirkby, 2003; Wicke *et al.*, 2011; FAO, 2015), with substantial repercussions on both natural (Thomas & Middleton, 1993; Lombardini, 2006; Zhou *et al.*, 2017) and managed ecosystems (Oldeman *et al.*, 1990; Rohades *et al.*, 1992; Jobbágy & Jackson, 2004; Marchesini *et al.*, 2017). Out of the 1.5 billion ha in use for crop production world-wide, human-induced (secondary) salinity is now impacting some 0.3 billion ha and already represents a threat to the food security of arid regions, where irrigation is employed routinely (Ghassemi *et al.*, 1995; Pitman & Läuchli, 2002). Projected climate change and associated sea-level rise, population growth, and increasing demand for water and crop production are expected to induce a further uptick in both natural (primary) and secondary salinization over the next decades (Pankova & Konyushkova, 2014; Qadir *et al.*, 2014; Jesus *et al.*, 2015; Daneshmand *et al.*, 2019). The fast growth of the salinization phenomenon thus calls for effective solutions to mitigate the different forms of salt-induced

land degradation. With salinization requiring global attention, salt-tolerant plants (*halophytes*) are becoming a significant component of current agro-ecosystems and natural ecosystem restoration practices promising to increase the overall food yield, enhance the resilience of traditional cropping, and contribute to efforts in reclaiming salt-affected soils (Boyko & Boyko, 1959; Epstein *et al.*, 1980; Qadir *et al.*, 1996, 2000; Ammari *et al.*, 2008; Munns & Gilliam, 2015).

The general mechanisms by which plants respond to soil salinity are quite well-known and have been studied for more than half a century (Longstreth & Nobel, 1979; Yeo *et al.*, 1985; García-Legaz *et al.*, 1993; Steduto *et al.*, 2000; Chartzoulakis *et al.*, 2002; Barr, 2005; Kathilankal *et al.*, 2008; Yarami & Sepaskhah, 2015). At the whole-plant scale, salinity largely affects the yield by limiting (1) water movement from the soil to the leaf, (2) CO<sub>2</sub> uptake in the leaf, and (3) carbohydrate production and its translocation in the phloem to satisfy the plant's carbon sinks. However, progress in how to link xylem–leaf–phloem transport mechanisms in response to salt stress remains in its embryonic state (Munns & Termaat, 1986; Bui, 2013; Negrão *et al.*, 2017; Perri *et al.*, 2018a) and represents a necessary step toward addressing the future role of

halophytes in managed and natural ecosystems. Understanding the interactions between vegetation and salinity is also becoming necessary to assess land–climate interactions in drylands where soil salinization is widespread (Hirschi *et al.*, 2011; Volpe *et al.*, 2011; Miralles *et al.*, 2012; Casagrande *et al.*, 2015; Good *et al.*, 2017; Kumar *et al.*, 2017).

The combined effects of salinization and projected CO<sub>2</sub> enrichment could furthermore affect plant water and carbon use strategies for now and the foreseeable future (Langley & Megonigal, 2010; Fatichi *et al.*, 2016, 2019; Wendelberger & Richards, 2017; Perri *et al.*, 2018b). A prominent example comes from coastal ecosystems such as mangroves and tidal wetlands, where sea-level rise and saltwater intrusion already exert significant controls on species shifts and carbon balance at the ecosystem level (Alongi, 1998; Kirwan *et al.*, 2010; Herbert *et al.*, 2015; Wendelberger & Richards, 2017).

Herein, the working hypothesis is that the response of different species to salt exposure is related to their ability in regulating the concentration of osmolytes in the xylem–leaf–phloem system. Building on this assumption, a physically based model that represents the short-term impacts of salinity on plant–water relations and xylem–leaf–phloem hydraulic coupling is proposed. The approach relies on (a) the cohesion–tension theory in the root–plant system, (b) the balance between biochemical demand and atmospheric supply of carbon dioxide (CO<sub>2</sub>) at the leaf, and (c) the Münch osmoregulation theory for carbohydrate movement in the phloem.

The combination of these theories captures the key pathways by which salinity and atmospheric CO<sub>2</sub> concentration impact plant productivity on short timescales (i.e. much shorter than timescales over which morphological adaptations occur in response to salt stress). However, even within this restricted framework, the combination of these theories remains mathematically unclosed and necessitates an additional constraint that relates soil salinity to leaf water potential ( $\psi_l$ ). Four different ‘closure’ assumptions are here explored to supplement the coupled CO<sub>2</sub>–water–carbohydrate transport equations in the xylem–leaf–phloem system. The main premise is that plants evolved to instantaneously maximize either (1) sap flow sustaining leaf turgor, (2) leaf CO<sub>2</sub> assimilation, (3) carbohydrate (mainly sucrose) production and loading, or (4) the difference between carbon gain and hydraulic cost. These four differing arguments are summarized in Table 1 and discussed in the Materials and Methods section. Each hypothesis can be viewed as an independent mathematical closure scheme enabling a solution to the combined cohesion–tension theory, Münch osmoregulation theory for carbohydrate movement in the phloem, and balance between biochemical demand and atmospheric supply of CO<sub>2</sub>. Such optimality schemes are intended to replace the empirical estimation of stomatal conductance previously used in studies exploring the hydraulic aspect of salt tolerance (Perri *et al.*, 2017, 2018a).

The objective is to compare the carbon–water–sucrose relations obtained from these four maximization schemes when combined with a common set of equations describing the xylem–leaf–phloem transport laws. This comparison allows assessing which maximization scheme imposes the largest constraint on

**Table 1** Summary of the four optimality hypotheses and relevant bibliography.

Hypothesis	Formulation	References
(1) Water uptake maximization: plants have evolved to maximize water transport from the soil to the leaves and maintain elevated cells turgor	$\frac{\partial f_{es}}{\partial \psi_l} = 0$	Begg & Turner (1976); Morgan (1984); Meinzer & Grantz (1990); Sperry <i>et al.</i> (1998); Sperry (2000)
(2) CO <sub>2</sub> maximization: stomatal regulation is performed to maximize carbon gain for given soil and atmospheric conditions	$\frac{\partial f_c}{\partial \psi_l} = 0$	Cowan & Farquhar (1977); Cowan (1982); Hari <i>et al.</i> (1986); Damour <i>et al.</i> (2010); Katul <i>et al.</i> (2010); Medlyn <i>et al.</i> (2011); Manzoni <i>et al.</i> (2011); Novick <i>et al.</i> (2016); Buckley <i>et al.</i> (2017); Paschalis <i>et al.</i> (2017)
(3) Sucrose transport maximization: plants regulate leaf water potential to maximize sucrose transport from the source (leaf) to the sink (root)	$\frac{\partial F_s}{\partial \psi_l} = 0$	Nikinmaa <i>et al.</i> (2013, 2014); Hölttä <i>et al.</i> (2017); Huang <i>et al.</i> (2018); Konrad <i>et al.</i> (2018)
(4) Profit maximization: evolutionary strategies in water-competitive environment lead to the maximization of carbon gain minus hydraulic risk	$\frac{\partial}{\partial \psi_l} (G - \mathcal{R}) = 0$	Anderegg <i>et al.</i> (2017, 2018); Sperry <i>et al.</i> (2017); Venturas <i>et al.</i> (2017, 2018); Eller <i>et al.</i> (2018); Love <i>et al.</i> (2019); Venturas <i>et al.</i> (2018)

plant–water relations. It also enables us to explain the observed plant response, in terms of transpiration, photosynthesis, leaf water potential, amongst other parameters, to increasing salinity. The focus is on well-watered conditions as may be expected in irrigated agro-ecosystems or coastal marshes so that salt concentration in the soil can be assumed to be the main cause of plant stress and is treated as the primary control parameter.

The proposed framework is able to account for salinity in the soil and within the plant, allowing the evaluation of the impacts of salt concentration on plant gross primary productivity across different levels of plant salt tolerance. Osmoregulation is shown to be the main factor determining the different response to short-term salinity exposure exhibited by halophytes and glycophytes (i.e. salt-sensitive species). While salt-tolerant plants show a different osmoregulatory response to salt and water stress, salt sensitivity results in the implementation of similar strategies to contrast droughts and salt exposure. The framework is then used to offer conjectures about possible ‘stress-mitigation effects’ of elevated atmospheric CO<sub>2</sub> enrichment for both salt-tolerant and salt-sensitive species.

## Materials and Methods

When subjected to water stress, isohydric plants regulate leaf water potential ( $\psi_l$ ) so as to achieve certain goals such as

avoiding: (1) embolism in the xylem (Salleo *et al.*, 2000; Lampinen & Noponen, 2003; Sobrado, 2007; Meinzer *et al.*, 2009), (2) reductions in carbohydrates production and transport (Farquhar *et al.*, 1980; Chaves, 1991; Flexas & Medrano, 2002; Flexas *et al.*, 2004; Tyerman *et al.*, 2019), and (3) losses of leaf turgor. These goals are similar to the ones of plants under short-term salinity exposure and represent the dominant strategy for responding to osmotic stress (Munns, 2002). However, in the context of drought stress, plants have mainly evolved to avoid xylem cavitation thereby maximizing water-saving (Pickard, 1981; Tyree & Sperry, 1989; Sperry, 2000; Cochard, 2006; Uri *et al.*, 2013). By contrast, the response to salt stress is based on maintaining optimal internal salt concentration, and could therefore lead to less conservative water strategies.

The aforementioned goals can be broadly expressed as four differing maximization hypotheses that form the basis of the approach used here to investigate salt stress, and contrast salt and drought tolerance. The first is a classical representation that assumes plants maximize water transport from the soil to maintain leaf turgor and elevated stomatal conductance (Begg & Turner, 1976; Turner & Jones, 1980; Morgan, 1984; Meinzer & Grantz, 1990; Sperry *et al.*, 1998; Comstock & Sperry, 2000; Sperry, 2000). The second postulates that plants maximize CO<sub>2</sub> uptake for a fixed amount of initial soil water available in the root zone per unit of leaf area (Cowan & Farquhar, 1977; Cowan, 1982; Hari *et al.*, 1986; Damour *et al.*, 2010; Katul *et al.*, 2010; Manzoni *et al.*, 2011, 2013a; Medlyn *et al.*, 2011; Volpe *et al.*, 2011; Novick *et al.*, 2016; Buckley *et al.*, 2017; Paschalis *et al.*, 2017). This assumption translates into the well-studied stomatal optimization theories (SOT) and economics of leaf-gas exchange for well-watered conditions. The SOT in Cowan & Farquhar (1977), as well as most schemes optimizing CO<sub>2</sub> assimilation rate, consider a constrained maximization (based on available water) that is then converted into an unconstrained optimization using the Lagrange multiplier approach (Manzoni *et al.*, 2013a).

In the case of salinity effects on plants, water availability is not necessarily a limiting factor, although water uptake increases salinity in the leaf thereby acting as a 'cost' to the carbon economy of the plant (Volpe *et al.*, 2011). More recently, it has been suggested that sucrose transport can impose a severe constraint on leaf-level gas exchange (Hölttä *et al.*, 2006; Mencuccini & Hölttä, 2010; Nikinmaa *et al.*, 2013; Jensen *et al.*, 2016). Carbohydrates are an essential component for metabolic maintenance and biomass production (Sánchez *et al.*, 1998; Cannell & Thornley, 2000; Runyan & D'Odorico, 2010). The third hypothesis thus assumes that plants regulate  $\psi_l$  to maximize sucrose transport from the source (leaf) to the sinks (roots and other plants organs; Hölttä *et al.*, 2017; Huang *et al.*, 2018; Konrad *et al.*, 2018).

Finally, the fourth hypothesis is based on the assumption that stomatal opening is adjusting instantaneously to maximize the difference between carbon gain and hydraulic cost (profit-maximization theory; Sperry *et al.*, 2016, 2017; Wolf *et al.*, 2016; Anderegg *et al.*, 2017, 2018; Venturas *et al.*, 2017, 2018; Love *et al.*, 2019). Profit-maximization approaches are now being popularized in studies of plant response to extended droughts, thereby offering an

alternative to conventional optimization schemes such as SOT (Mencuccini *et al.*, 2019, and references therein). However, the utility of profit maximization schemes to saline environments has not been undertaken in previous studies and constitutes one of the main novelties here. To compare these differing optimization arguments in a consistent manner, leaf water potential is selected as the 'control variable'. The  $\psi_l$  is constrained to be always smaller than the soil potential. Water and mass fluxes in the xylem–leaf–phloem are all expressed as a function of leaf water potential subject to the constraint mentioned above.

The proposed framework aims at describing the effects of increasing soil salinity on both halophytes and glycophytes. The impacts of salt are included in the soil water potential that is assumed to be dominated by the osmotic component of salt stress for well-watered or irrigated conditions. Salinity increases in the plant as a result of salt water uptake from the soil (Scholander *et al.*, 1966; Scholander, 1968; Glenn *et al.*, 1999; Khan *et al.*, 2000) until a 'chemical-equilibrium' is attained between leaf and soil salt concentration (see section 'Plant water flux'). When such equilibrium is reached, filtration theory can be used to link leaf to soil salt concentration using simplified models of filtration efficiency. To reduce the large manifold of possible scenarios and parameters to be explored, the four differing mathematical closure schemes are contrasted here at the incipient point when chemical equilibrium is achieved. The transient phase associated with the attainment of such chemical equilibrium is kept for a future study.

## Theoretical framework

To maintain model simplicity, a mono-species well-irrigated stand is considered. The elevated soil moisture in the rooting zone is maintained using irrigated saline water with prescribed salt concentration. Soil moisture and soil salt concentration are assumed to be uniform across the entire rooting zone. The stand density is assumed to be below the incipient point of overcrowding, and leaf area index represents the surface area responsible for photon capture and concomitant leaf gas exchange with the atmosphere.

A conceptual representation of water, carbon and sucrose transport illustrating key interconnections between plant compartments is presented in Fig. 1. The driving force for water and CO<sub>2</sub> movement in the soil plant system arises from their concentration difference relative to the atmosphere (sections 'Plant water flux' and 'CO<sub>2</sub> assimilation rate'). Sucrose is produced by photosynthesis and transported from the mesophyll to the phloem (Giaquinta, 1983; Rennie & Turgeon, 2009; Hölttä *et al.*, 2017). Here it is translocated from the source (leaf) to the sink (root) as a result of osmotic gradients (diffusive or osmotically-driven transport) and as a consequence of water movement from the xylem to the phloem (advective transport; see section 'Sucrose transport').

It is known that water flow in the phloem is at least one order of magnitude smaller than water flux in the xylem (Jensen *et al.*, 2016). Transpiration responds instantaneously and proportionally to fluctuations in the external forcing, whereas sap flow response displays a time delay. As a consequence, when the model is solved for short timescales for leaf water potential,

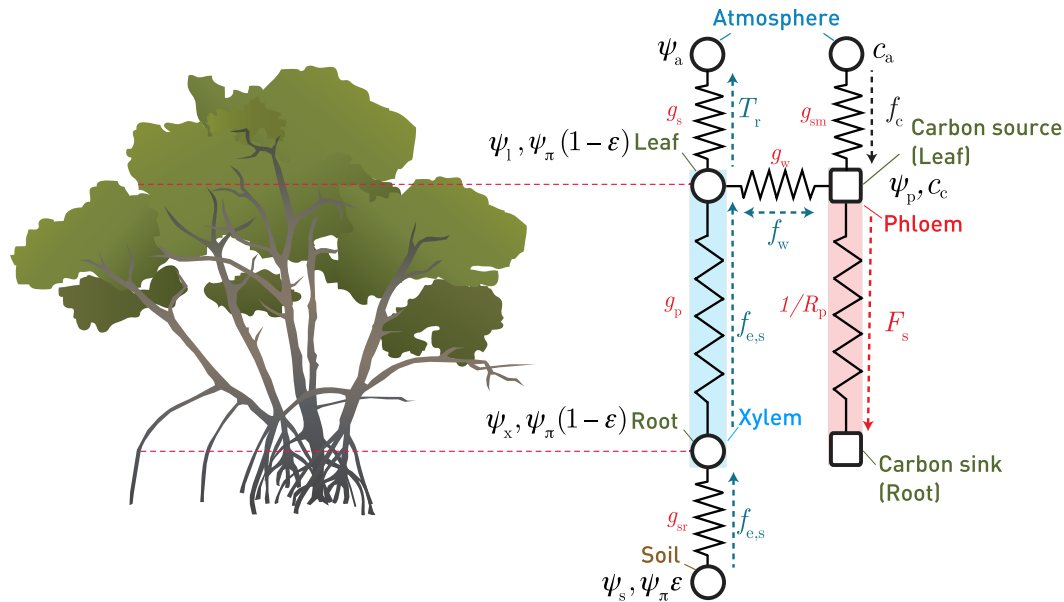


**Fig. 1** Conceptual representation of water transport in the xylem, and sucrose transport in the phloem as regulated by leaf-level gas exchange. Symbols are defined in Table 1. *Rhizophora mangle* outline is courtesy of the Integration and Application Network, University of Maryland Center for Environmental Science (ian.umces.edu/symbols/).

the phloem can be assumed to act as local storage of water and salt. This timescales mismatch also implies that a Münch counter-flow is negligible in this framework. Steady-state conditions inside each leaf are assumed, so that supply from the atmosphere balances the biochemical demand for carbon dioxide. Each  $\text{CO}_2$  molecule that enters through stomata is assimilated in the mesophyll and then used for sucrose production. Hence, the model assumes that sucrose production inside the leaf occurs proportionally to photosynthesis at a rate that varies with phloem geometric factors and whether sucrose loading is passive or active. The mesophyll conductance (or, better, its diffusive properties) is assumed to respond instantaneously to  $\psi_l$  as discussed elsewhere (Dewar *et al.*, 2018). Hence, salinity directly affects the photosynthetic pathway in addition to limiting stomatal and xylem conductance through  $\psi_l$ .

**Plant water flux** Assuming continuity in the water potential (Nobel, 1983), the transpiration flux per unit of ground surface area  $T_r$  is given by the difference between plant water supply or uptake  $f_{e,s}$  and water flux to the phloem  $f_w$ :

$$T_r = f_{e,s} - f_w. \quad \text{Eqn 1}$$

Plant water uptake depends on plant hydraulic characteristics and is expressed as a function soil–root–plant conductance  $g_{srp}$  and the water potential gradient between soil  $\psi_{\text{tot}}$  and  $\psi_l$ :

$$f_{e,s} = g_{srp}(\psi_{\text{tot}} - \psi_l). \quad \text{Eqn 2}$$

The total soil water potential  $\psi_{\text{tot}}$  is the sum of matric  $\psi_s$  and osmotic potential  $\psi_\pi$ . Soil matric potential becomes more negative as the relative soil moisture  $s$  is reduced, where  $s$  is defined by the ratio of actual root-zone soil moisture content and soil porosity.

The functional relation between  $\psi_s$  and  $s$  can be described using conventional soil water retention curves (Buckingham, 1907; Clapp & Hornberger, 1978) in the form  $\psi_s = \psi_{ss} s^{-m}$ , where  $\psi_{ss}$  is the soil water potential near field saturation and  $m$  is a parameter accounting for the curvature of the retention curve. The actual osmotic water potential depends on the molar salt concentration in the soil water  $C$  and is given by the van't Hoff equation:  $\psi_\pi = \epsilon C R i_v T_w$ , where  $\epsilon$  is the root filtration efficiency,  $R$  is the universal gas constant,  $i_v$  is the van't Hoff coefficient for NaCl, and  $T_w$  is the soil water temperature. Filtration efficiency  $\epsilon$  is assumed to be a linearly increasing function of  $C$  given by  $\epsilon = a + bC$ , where  $a$  is the filtration efficiency when  $C$  approaches 0 (clean water), and  $b$  is the rate of efficiency increment with salinity (see Perri *et al.*, 2017, 2018a, and Supporting Information Notes S1). It has been assumed that filtration at the root level occurs analogously to a membrane (or cross-flow) filtration. Accordingly, salt removal is driven by the gradient in water potential between the soil and the xylem. The filtration efficiency accounts for the fact that salt is not completely removed at the root level and a certain amount of ions can enter the plant (Parida & Jha, 2010).

The series of the soil–root ( $g_{sr}$ ) and plant ( $g_p$ ) conductances defines  $g_{srp} = \frac{\text{LAI} g_{sr} g_p}{\text{LAI} g_p + g_{sr}}$ , with LAI being the leaf area index (leaf area per unit ground area). The conductance  $g_{srp}$  is re-scaled to LAI to express the water uptake per unit of ground area (see Notes S2). An effective vulnerability curve is used to represent xylem cavitation due to reduced leaf water potential and is given by (Sperry *et al.*, 1998):

$$g_p = g_{p,\text{max}} \exp\left(\frac{\psi_l}{d}\right)^c, \quad \text{Eqn 3}$$



where  $g_{p,\max}$  is the maximum plant conductance,  $d$  and  $c$  are parameters determined such that  $g_p$  approaches 0 for the most negative values of  $\psi_l$  and is equal to  $g_{p,\max}$  for  $\psi_l = 0$ .

The water flux from the xylem to the phloem  $f_w$  can be estimated as a function of water potential gradient at the interface between xylem and phloem, and depends on water permeability and area of the xylem–phloem interface. The characteristics of this membrane are modeled using the hydraulic conductance at the interface  $g_w$ , which varies as a function of water potential with a relation analogous to Eqn 3. The flux  $f_w$  is hence given by (Bartlett *et al.*, 2014; Perri *et al.*, 2018a):

$$f_w = g_w \text{LAI}(\psi_l - \psi_p), \quad \text{Eqn 4}$$

where  $\psi_p$  is the phloem water potential arising from the sum of osmotic pressure due to the concentration of molar sucrose  $C_s$  and salt  $C_p$  (i.e.  $\psi_p = RT_p(i_{v,s}C_s + i_{v,p}C_p)$ , with  $i_{v,s}$  being the van't Hoff coefficient for sucrose and  $T_p$  the phloem temperature assumed to be equal to leaf temperature  $T_l$ ). The turgor term (positive) of phloem water potential has been neglected here, observing that it is orders of magnitude smaller than the osmotic component (negative). This assumption is realistic for nonsucculent plants considering that the volume of water in the phloem is relatively small compared with the one of the xylem, whereas phloem ion concentration is extremely high (Jensen *et al.*, 2016). By contrast, turgor pressure terms cannot be considered negligible for succulent species (Ranney *et al.*, 1990; Bartlett *et al.*, 2014).

At steady-state, the plant water supply in Eqn 2 must be balanced by the water loss to the atmosphere  $f_{e,d}$ . Assuming that cuticular transpiration (direct diffusion of water vapor through external membranes; Riederer & Muller, 2008) is negligible compared to the water flux through the stomata, the water loss to the atmosphere must be proportional to the stomatal conductance  $g_s$  and the vapor pressure gradient between the leaf  $e_l$  and the atmosphere  $e_a$  and can be expressed as (Nobel, 1983; Daly *et al.*, 2004):

$$f_{e,d} = g_s \frac{\text{MW}_{\text{ratio}}}{p_0} (e_l - e_a), \quad \text{Eqn 5}$$

where  $p_0$  is the atmospheric pressure and  $\text{MW}_{\text{ratio}}$  is the water to dry-air molecular weight ratio.

Stomatal conductance can be obtained by equating Eqns 2 and 5 to yield:

$$g_s = g_{\text{stp}} \frac{p_0(\psi_{\text{tot}} - \psi_l)}{\text{MW}_{\text{ratio}}(e_l - e_a)}. \quad \text{Eqn 6}$$

The system of Eqns 1–6 requires  $\psi_l$  to be determined and depends on the sucrose concentration in the phloem (through Eqn 4). The latter is obtained by coupling the plant hydraulics to  $\text{CO}_2$  assimilation and sucrose transport as featured next.

**$\text{CO}_2$  assimilation rate** The prevailing metabolic pathway among glycophytes and halophyte is  $\text{C}_3$  photosynthesis, from

which our choice to focus on  $\text{C}_3$  plants. The  $\text{CO}_2$  biochemical demand ( $=f_{c,d}$ ) is thus obtained through the Farquhar photosynthesis model (Farquhar *et al.*, 1980):

$$f_{c,d} = \frac{k_1(c_c - \Gamma^*)}{k_2 + c_c} - R_d, \quad \text{Eqn 7}$$

where  $c_c$  is the chloroplast  $\text{CO}_2$  concentration,  $k_1$  and  $k_2$  are photosynthetic parameters that vary with photosynthetically active radiation (PAR) and leaf temperature,  $\Gamma^*$  is the  $\text{CO}_2$  compensation point in the absence of mitochondrial respiration, and  $R_d$  is the daytime respiration rate. The parameters  $k_1$  and  $k_2$  are defined depending on whether photosynthesis is Rubisco or Ribulose biphosphate (RuBP) limited (see Collatz *et al.*, 1991; Medlyn *et al.*, 2002; Vico *et al.*, 2013).

To satisfy the plant biochemical demand,  $\text{CO}_2$  is supplied from the atmosphere into the intercellular space within the leaf. The supply rate  $f_{c,s}$  is driven by the  $\text{CO}_2$  concentration difference between the atmosphere and the leaf and is regulated by the stomatal conductance to  $\text{CO}_2$ ,  $g_{s,\text{CO}_2}$ :

$$f_{c,s} = g_{s,\text{CO}_2}(c_a - c_i) = g_m(c_i - c_c), \quad \text{Eqn 8}$$

where  $c_a$  and  $c_i$  are atmospheric and intercellular  $\text{CO}_2$  concentrations, respectively, and  $g_m$  is the mesophyll conductance. The conductance  $g_{s,\text{CO}_2}$  can be estimated from  $g_s$  as  $g_{s,\text{CO}_2} = g_s/r$  where  $r \approx 1.6$  is the relative molecular diffusivity of water vapor with respect to  $\text{CO}_2$ . From Eqn 8, the  $\text{CO}_2$  supply can be expressed as  $f_{c,s} = g_{s,m}(c_a - c_c)$ , where  $g_{s,m}$  is given by the series of stomatal and mesophyll conductances:  $g_{s,m} = g_{s,\text{CO}_2}g_m / (g_{s,\text{CO}_2} + g_m)$ . Using a recent formulation proposed by Dewar *et al.* (2018), the ratio between chloroplast and intercellular  $\text{CO}_2$  concentration is governed by a stress function at the leaf level,  $\theta(\psi_l)$ , which represents a reduction factor depending on  $\psi_l$  and the critical leaf water potential,  $\psi_c$ . A plausible model for  $\theta$  is given by  $\theta(\psi_l) = 1 - \frac{\psi_l}{\psi_c}$ . The parameter  $\psi_c$  represents the value of  $\psi_l$  at which stomatal and mesophyll conductance are completely impaired. Dewar *et al.* formulation may be simplified to yield:

$$\frac{c_c}{c_i} = \frac{\Gamma^* + c_i\theta(\psi_l) - \Gamma^*\theta(\psi_l)}{c_i}. \quad \text{Eqn 9}$$

Eqn 9 accounts for the fact that at low  $\psi_p$  the  $\text{CO}_2$  concentration is lower in the chloroplast than in the intercellular space so that  $c_c < c_i$ . Thus, Eqn 9 describes the reduction in mesophyll conductance due to salt stress and the consequent decline in photosynthetic capacity. Regardless of the  $\psi_l$  value, the  $c_c$  is constrained by the value of  $c_i$  at the  $\text{CO}_2$  compensation point  $\Gamma^*$ .

The  $f_c$  can be obtained by solving the system of Eqns 7–9 assuming that the biochemical demand balances the atmospheric supply of  $\text{CO}_2$ . This assumption leads to:

$$f_c = \frac{1}{2\theta} [g_{s,\text{CO}_2}(k_2 + \theta^*) + \theta(k_1 - R_d) - \Theta], \quad \text{Eqn 10}$$

where  $\Theta$  is given by:

$$\Theta = \sqrt{4g_{s,CO_2} [k_2 g_{s,CO_2} \theta^* + \theta(k_2 R_d + \Gamma^* k_1)] + [g_{s,CO_2} (k_2 - \theta^*) + \theta(k_1 - R_d)]^2}, \quad \text{Eqn 11}$$

and  $\theta^* = \theta(c_a - \Gamma^*) + \Gamma^*$ . In Eqn 10, the  $f_c$  does not depend on  $c_c$  or  $c_i$ . It is a function of  $\psi_l$  for specified soil vegetation characteristics and external environmental conditions. Also, the photosynthetic capacity is a function of  $T_b$  which is commonly assumed to be approximately equal to ambient air temperature  $T_a$  (well-coupled leaf-to-atmosphere conditions).

However, in arid or salt-affected ecosystems,  $T_l$  can be significantly higher than  $T_a$  due to elevated incident radiation and scarce evaporative cooling (i.e. leaf transpiration is limited). To account for this effect, an energy balance at the leaf-level is applied based on a 'big leaf approximation' to yield  $T_l = T_a + (\phi - T_r \Delta H_{vap} \rho_w) / (\rho g_a c_p)$ , where  $\phi$  is the net radiation,  $\Delta H_{vap}$  is the latent heat of vaporization of water,  $c_p$  is the air isobaric specific heat capacity,  $\rho_w$  is the water density,  $\rho$  is the mean air density and  $g_a$  is the aerodynamic conductance estimated using conventional flow over flat-plate theory (Sinclair *et al.*, 1976; Dingman, 2015; Perri *et al.*, 2017).

**Sucrose transport** It is assumed that the main carbohydrate produced by photosynthesis is sucrose ( $C_{12}H_{22}O_{11}$ ), which is rapidly transported into the loading zone. Over short timescales (sub-hourly), atmospheric forcing and soil water conditions are approximately stationary. Consequently, the production rate of sucrose ( $P_C$ ) in the loading zone can be defined as  $P_C \approx \alpha(\beta f_c LAI)$ , where  $\alpha$  is a species-specific loading efficiency factor, and  $\beta = 1/12$  is the number of sucrose molecules produced for each molecule of  $CO_2$  assimilated (Huang *et al.*, 2018). Within the loading zone,

$$\frac{d(V_p C_s)}{dt} = P_C - U_C = \alpha(\beta f_c LAI) - U_C, \quad \text{Eqn 12}$$

where  $C_s$  is the sucrose concentration,  $U_C$  is the sucrose removal rate from the loading cell, and  $V_p$  is the volume of loading cell assumed to be constant. A model of maximum simplicity for  $U_C$  can be obtained in analogy to first-order kinetics so that  $U_C = C_s / \tau$ , where  $\tau$  is a characteristic timescale (or inverse-removal rate constant) related to the production-to-transport process (typically ~ minutes to hours) per unit of phloem volume (Huang *et al.*, 2018).

At steady-state,  $d(V_p C_s)/dt = 0$  and the concentration of sucrose in the phloem loading zone (leaf) can be related to the source or production rate using  $C_s = P_C \tau$ . The sucrose transport rate within the phloem, considering both advective and diffusive (osmotically driven) transport, is then given by:

$$F_s = C_s f_w + \frac{(\psi_p + \Delta p)}{R_p}, \quad \text{Eqn 13}$$

where  $\Delta p = (\psi_l - \psi_{\text{tor}})$  is the xylem pressure difference between sucrose source (leaf) and sink (soil root), and  $R_p$  is the total plant resistance to sucrose transport (Konrad *et al.*, 2018). The resistance  $R_p$  depends on the geometry of the phloem and the viscosity of the sap and is given by (Jensen *et al.*, 2016):

$$R_p(C_s) = \eta(C_s) \mathcal{L}, \quad \text{Eqn 14}$$

where  $\mathcal{L}$  is a geometric factor depending on phloem morphology. The sap viscosity increases nonlinearly with sucrose concentration using the approximate expression  $\eta(C_s) = \eta_w \exp(b_1 C_s - b_2 C_s^2 + b_3 C_s^3)$ , where  $\eta_w$  is the dynamic viscosity of pure water, and  $b_1$ ,  $b_2$  and  $b_3$  are empirical parameters providing the best fit to observed functional relations between  $\eta$  and  $C_s$  (not repeated here). Table 2 reports the list of variables and units used throughout the text.

**Optimality hypotheses and mathematical closure assumptions** Up to this point, water transport from the soil to the leaf, photosynthesis, and sucrose production in the leaf are all expressed as a function of  $\psi_l$ . To proceed further, one additional equation is needed to determine  $\psi_l$ . The four differing maximization hypotheses are then used to reach a mathematical closure enabling the determination of  $\psi_l$ . They are expressed as:

$$\begin{cases} \frac{\partial f_c}{\partial \psi_l} = 0 & (a) \\ \frac{\partial f_c}{\partial \psi_l} = 0 & (b) \\ \frac{\partial F_s}{\partial \psi_l} = 0 & (c) \\ \frac{\partial}{\partial \psi_l} (\mathcal{G} - \mathcal{R}) = 0 & (d) \end{cases}, \quad \text{Eqn 15}$$

where  $\mathcal{G} = (f_c / f_{c,\text{max}})$  is the relative carbon gain and  $\mathcal{R} = (1 - g_p / g_{p,\text{max}})$  is the hydraulic risk. Eqn 15 is solved to find  $\psi_l$  either by maximizing water uptake (Eqn 15a), carbon assimilation rate (Eqn 15b), sucrose transport (Eqn 15c) or carbon profit (Eqn 15d) as a function of soil salinity. The solution is obtained at steady-state and in well-watered conditions assuming constant plant morphological traits (short-term salinity exposure; Perri *et al.*, 2018a). Further assumptions and model limitations are described in section 'Model limitations'.

## Meta-analysis and model parametrization

A multi species meta-analysis is conducted to obtain plausible photosynthetic model parameters for halophytes and glycophytes (with data obtained from: Bonghi & Loreto, 1989; Brugnoli & Lauteri, 1991; Lin & da S. L. Sternberg, 1993; Tattini *et al.*, 1997; Delfine *et al.*, 1998, 1999; Ahmed *et al.*, 2008; Razzaghi *et al.*, 2015). Published gas exchange measurements featuring  $f_c$  and  $g_s$  are used for this purpose (see Dataset S1; Table S1). As shown in Fig. 2(a), for a given stomatal conductance value, salt-sensitive plants display higher assimilation rate than tolerant ones. This follows from the fact that halophytes, growing in soils where water availability is generally not the main source of stress,

**Table 2** Nomenclature.

Symbol	Description	Unit
$C$	Soil salinity	$\text{mol m}^{-3}$
$C_p$	Salt concentration in the phloem	$\text{mol m}^{-3}$
$C_s$	Molar sucrose concentration in the phloem	$\text{mol m}^{-3}$
$c_a$	Atmospheric $\text{CO}_2$ concentration	ppm
$c_c$	$\text{CO}_2$ concentration in the chloroplast	ppm
$c_i$	Intercellular $\text{CO}_2$ concentration	ppm
$e_a$	Atmospheric water vapor pressure	MPa
$e_l$	Leaf water vapor pressure	MPa
$F_s$	Sucrose transport rate	$\mu\text{mol s}^{-1}$
$f_{c,d}$	$\text{CO}_2$ biochemical demand	$\mu\text{mol s}^{-1}$
$f_{c,s}$	$\text{CO}_2$ atmospheric supply	$\mu\text{mol s}^{-1}$
$f_{e,d}$	Atmospheric water demand	$\text{mmol s}^{-1}$
$f_{e,s}$	Plant water uptake	$\text{mmol s}^{-1}$
$f_w$	Xylem–phloem water flux	$\text{mmol s}^{-1}$
$G$	Carbon gain	Dimensionless
$g_m$	Mesophyll conductance	$\text{mmol s}^{-1}$
$g_p$	Plant conductance per unit of water potential	$\text{mmol MPa}^{-1} \text{ s}^{-1}$
$g_s$	Stomatal conductance	$\text{mmol s}^{-1}$
$g_{s,\text{CO}_2}$	Stomatal conductance to $\text{CO}_2$	$\text{mmol s}^{-1}$
$g_{s,m}$	Stomatal–mesophyll conductance	$\text{mmol s}^{-1}$
$g_{sr}$	Soil–root conductance per unit of water potential	$\text{mmol MPa}^{-1} \text{ s}^{-1}$
$g_{srp}$	Soil–root–plant conductance per unit of water potential	$\text{mmol MPa}^{-1} \text{ s}^{-1}$
$g_w$	Xylem–phloem conductance per unit of water potential	$\text{mmol MPa}^{-1} \text{ s}^{-1}$
$\mathcal{L}$	Phloem morphological parameter	$\mu\text{mol}^{-1}$
$P_C$	Sucrose production rate	$\mu\text{mol s}^{-1}$
$\mathcal{R}$	Hydraulic risk	Dimensionless
$R_p$	Resistance to sucrose transport	$\text{MPa s } \mu\text{mol}^{-1}$
$s$	Relative soil moisture	Dimensionless
$T_l$	Leaf temperature	K
$T_p$	Phloem water temperature	K
$T_r$	Transpiration flux	$\text{mmol s}^{-1}$
$U_C$	Sucrose removal rate	$\mu\text{mol s}^{-1}$
$V_p$	Volume of loading cell	$\text{m}^3$
$\varepsilon$	Filtration efficiency	Dimensionless
$\eta$	Viscosity of the sap	MPa s
$\theta$	Leaf-level stress function	Dimensionless
$\lambda$	Marginal water use efficiency	$\mu\text{mol mol}^{-1}$
$\psi_l$	Leaf water potential	MPa
$\psi_p$	Phloem water potential	MPa
$\psi_s$	Matric water potential	MPa
$\psi_{\text{tot}}$	Total soil water potential	MPa
$\psi_x$	Xylem water potential	MPa
$\psi_\pi$	Osmotic soil water potential	MPa

Defined per unit of ground area [ $\text{m}^2$ ]. See Supporting Information for details on flux and conductance definitions and units.

Defined per unit of leaf area [ $\text{m}^2$ ]. See Supporting Information for details on flux and conductance definitions and units.

are less water-efficient than drought-tolerant glycophytes (e.g. olives) under similar environmental conditions.

To now focus on two-end member plants representing different levels of salt tolerance, model parameterization has been performed using published measurements on *Rhizophora mangle* (salt-tolerant) and *Olea europea* (salt-sensitive). The model also has been parameterized for the highly tolerant species *Avicennia marina* and *Plantago maritima* with the goal of explaining the

different transpiration – salinity patterns observed in plants adapted to hypersaline environments. Soil, plant and photosynthetic parameters are extracted from published data (see Table 3; Pasioura *et al.*, 1992; Gómez *et al.*, 2001; Zarco-Tejada *et al.*, 2004; Tognetti *et al.*, 2007; Barr *et al.*, 2009; Manzoni *et al.*, 2013b), whereas the value of  $g_{p,\text{max}}$  and  $g_{w,\text{max}}$  are obtained by fitting observed and modeled  $f_c - g_s$  curves. Fig. 2 shows an example of modeled  $f_c$  as a function of  $g_s$  obtained while maximizing water uptake (b),  $\text{CO}_2$  assimilation (c) and sucrose transport (d). The model results are contrasted with measurements carried out by Barr *et al.* (2009) in a *R. mangle* forest. The expected  $f_c - g_s$  curves (solid lines) are in good agreement with the measured values for these three optimality closure hypotheses. Much of the variability in the data can be explained as a result of variations in ambient air temperature (not reported in Barr *et al.*'s experiments).

By contrast, the profit-maximization scheme well captures the behavior of glycophytes, whereas it overestimates the impact of salt stress in halophytes (see Fig. S1). The different performance of the scheme expressed in Eqn 15(d) is pinpointing the diverse water use strategies adopted by halophytes and glycophytes in coping with salinity. Table 3 reports the list of parameters used in the model calculations to be discussed in the Results section.

## Results

The effects of salinity on assimilation rate, sucrose transport and leaf water potential are explored here using model results from the four optimality closure schemes. The effects of soil salinity on the much-discussed marginal water use efficiency and apparent reductions in leaf carboxylation capacity are also presented. Nonstomatal limitations are included and are impacted by the decrease in leaf water potential associated with increasing soil salinity. Changes in apparent carboxylation capacity are primarily due to changes in mesophyll conductance (and relative plant conductance or  $c_c/c_i$ ).

### Effect of the optimality closure on plant-water relations

Fig. 3 shows leaf water potential (a,b), and relative plant conductance ( $g_p/g_{p,\text{max}}$ ; c,d) as a function of soil salinity for *R. mangle* (salt-tolerant) and *O. europea* (salt-sensitive). In *O. europea*, water uptake maximization implies a significantly lower leaf water potential when compared to the other three maximization rules. Also, the relative plant conductance decreases monotonically with increasing soil salinity with a faster decay for the maximization of water uptake. In *R. mangle*, water uptake,  $\text{CO}_2$  assimilation and sucrose transport maximization all lead to similar results in terms of  $\psi_l - C$  relation. Compared to the other three optimality schemes, profit-maximization results in higher (less negative) leaf water potential.

Fig. 4 shows transpiration rate (a,b) for *R. mangle* and *O. europea*, and a comparison between modeled and observed relative transpiration rate  $T_r/T_{r,\text{max}}$  (see Dataset S1; Table S2) in *R. mangle* (c), *O. europea* (d), *A. marina* (e), and *P. maritima* (f). The typical  $T_r - C$  nonmonotonic pattern previously observed in halophytes with a peak of  $T_r$  at intermediate salinity  $C_{\text{max}}$  (Ball

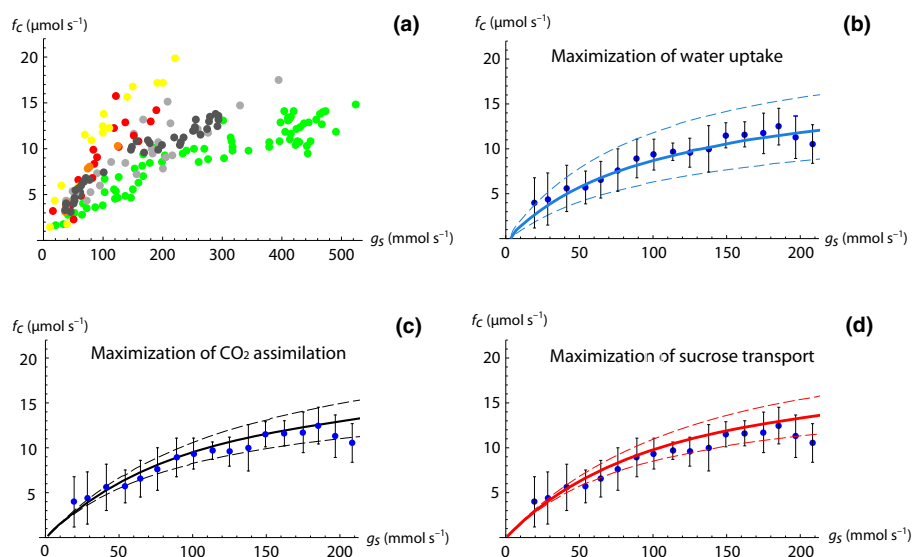


**Fig. 2** (a) Assimilation rate  $f_c$  as a function of water vapor stomatal conductance  $g_s$  across species with diverse salt tolerance traits. The species shown here, in decreasing order of salt tolerance, are: *Rhizophora mangle* L. (red mangrove; green; Lin & da S. L. Sternberg, 1993), *Chenopodium quinoa* Willd. (quinoa; light gray; Razzaghi *et al.*, 2015), *Gossypium hirsutum* L. (cotton; dark gray; Brugnoli & Lauteri, 1991), *Spinacia oleracea* L. (spinach; red; Delfine *et al.*, 1998, 1999), *Solanum lycopersicum* L. (tomato; orange; Haghighi & Pessarakli, 2013), and *Olea europaea* L. (olive; yellow; Bongio & Loreto, 1989; Tattini *et al.*, 1997; Ahmed *et al.*, 2008). (b–d)  $\text{CO}_2$  assimilation rate as a function of  $g_s$  for *R. mangle* obtained by (b) maximizing  $f_{e,s}$ , (c)  $f_c$ , and (d)  $F_s$ . Model results are compared to leaf-level measurements performed by Barr *et al.* (2009) (blue dots with the error bars representing  $\pm$  SD). Solid lines represent  $f_c - g_s$  at average ambient temperature, whereas dashed curves are obtained with temperature variations of  $\pm 5^\circ\text{C}$  with respect to the published mean air temperature value.

& Farquhar, 1984; Flanagan & Jefferies, 1989; Lin & da S. L. Sternberg, 1993; Takemura *et al.*, 2000) emerges here as a result of xylem–phloem interactions (Fig. 3e). In glycophyte, transpiration is a monotonically decreasing function of soil salt concentration (Fig. 3f). As expected, transpiration is considerably higher when plants adjust leaf water potential to maximize water uptake. It is to be noted that for halophytic species (Fig. 3a,c,d), sucrose

transport and carbon assimilation maximization schemes are the ones better reproducing the  $T_f$ – $C$  relation up to the optimal transpiration value. Above this value, water saving mechanisms become dominant also in halophytes. However, the dichotomy between maximization of productivity (up to  $C_{\text{max}}$ ) and water-saving (above  $C_{\text{max}}$ ) is more evident in woody plants, which are physiologically more reliant on osmoregulation.

**Table 3** Model parameters for *Rhizophora mangle* and *Olea europaea*.

Parameter	<i>Rhizophora mangle</i>	<i>Olea europaea</i>	Unit	Description
$\psi_{ss}$	$-1.43 \times 10^{-3}$	$-1.43 \times 10^{-3}$	MPa	Matric potential at saturation
$m$	5.4	5.4	–	Exponent of the retention curve
$i_v$	2	2	–	van't Hoff coefficient for NaCl
$i_{v,s}$	1	1	–	van't Hoff coefficient for sucrose
$a$	0.9	0.9	–	Filtration efficiency parameter
$b$	$10^{-4}$	$10^{-4}$	$\text{m}^3 \text{mol}^{-1}$	Filtration efficiency parameter
LAI	4.5	2.5	$\text{m}^2 \text{m}^{-2}$	Leaf area index
$g_{p,\text{max}}$	24.44	49.45	$\text{mmol MPa}^{-1} \text{s}^{-1}$	Maximum plant conductance
$g_{w,\text{max}}$	1.67	0.72	$\text{mmol MPa}^{-1} \text{s}^{-1}$	Maximum xylem–phloem conductance
$c$	3	3	–	Vulnerability curve exponent
$d$	3	3	MPa	Vulnerability curve parameter
$C_p$	150	150	$\text{mol m}^{-3}$	Phloem salt concentration
$\Gamma^*$	34.6	34.6	$\mu\text{mol mol}^{-1}$	$\text{CO}_2$ compensation point
$V_{c,\text{max}}$	76.15	80	$\mu\text{mol m}^{-2} \text{s}^{-1}$	Maximum carboxylation rate at $T_0 = 293.2 \text{ K}$
$\psi_c$	–3.5	–2.5	MPa	Critical leaf water potential
$R_d$	1.62	1.62	$\mu\text{mol s}^{-1}$	Daytime respiration rate
$\alpha$	1	1	–	Sucrose loading efficiency
$\beta$	1/12	1/12	$\mu\text{mol } \mu\text{mol}^{-1}$	$\text{CO}_2$ –sucrose stoichiometric ratio
$\tau$	0.35	0.63	$\text{s mm}^{-1}$	Characteristic timescale per unit of phloem volume
$b_1$	0.035	0.035	–	$\eta - C_s$ parameter
$b_2$	0.012	0.012	–	$\eta - C_s$ parameter
$b_3$	0.023	0.023	–	$\eta - C_s$ parameter

Defined per unit of leaf area [ $\text{m}^2$ ]. See Supporting Information for details on conductance definitions and units.



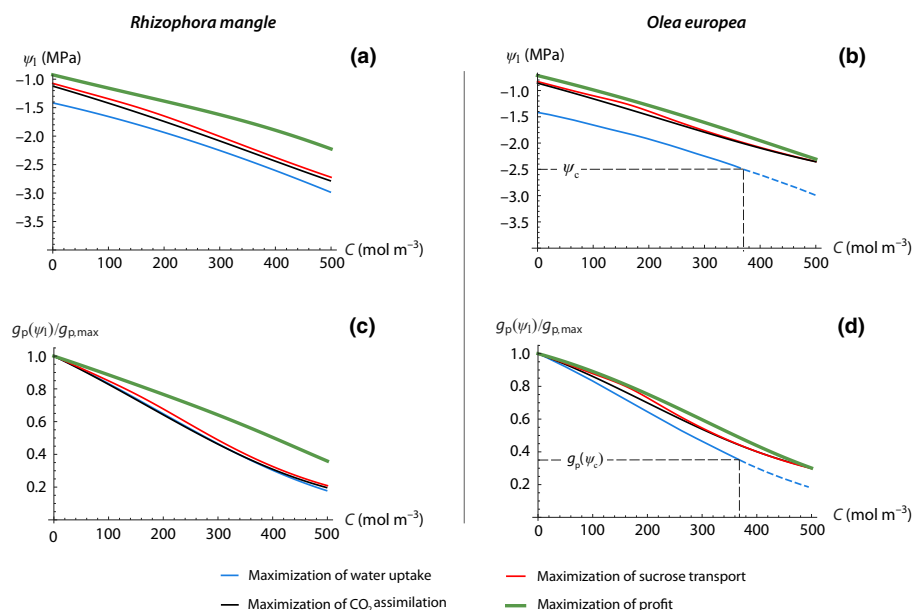
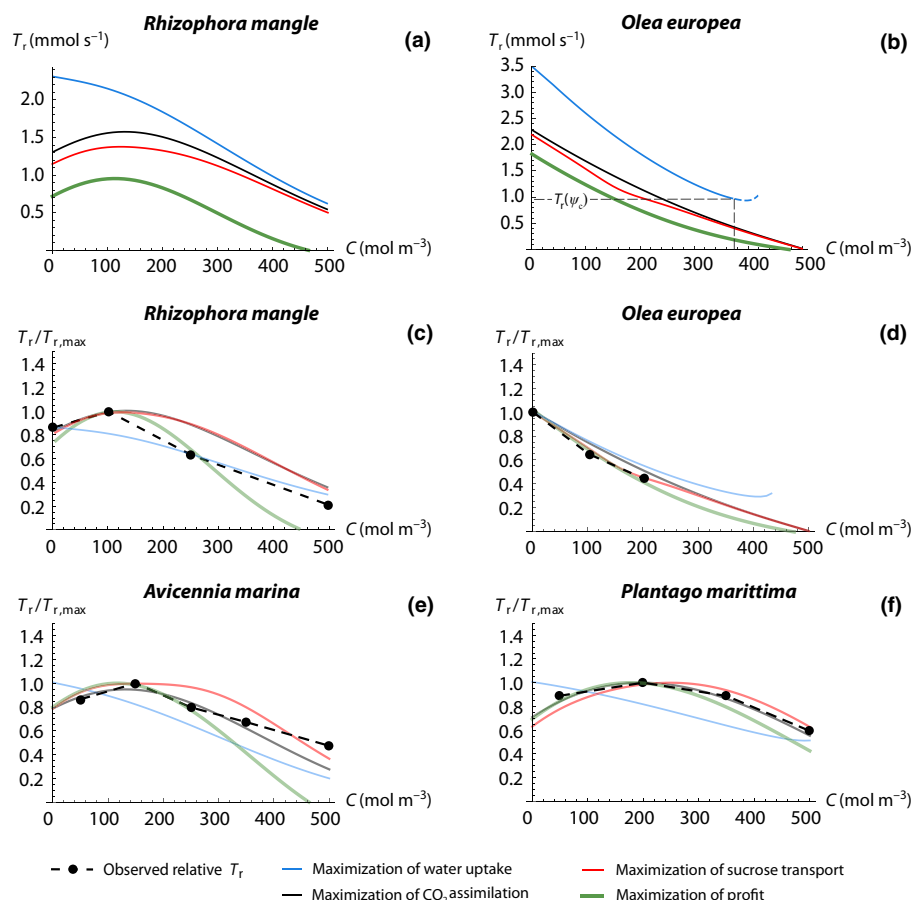


**Fig. 3** (a, b) Leaf water potential  $\psi_l$ , and (c, d) relative plant conductance  $g_p(\psi_l)/g_{p,max}$  as a function of soil salinity  $C$  as obtained from the four optimality rules for *Rhizophora mangle* (salt-tolerant) and *Olea europea* (salt-sensitive). Dashed lines represent unphysical values obtained for  $\psi_l \leq \psi_c$ , for which cavitation becomes dominant.

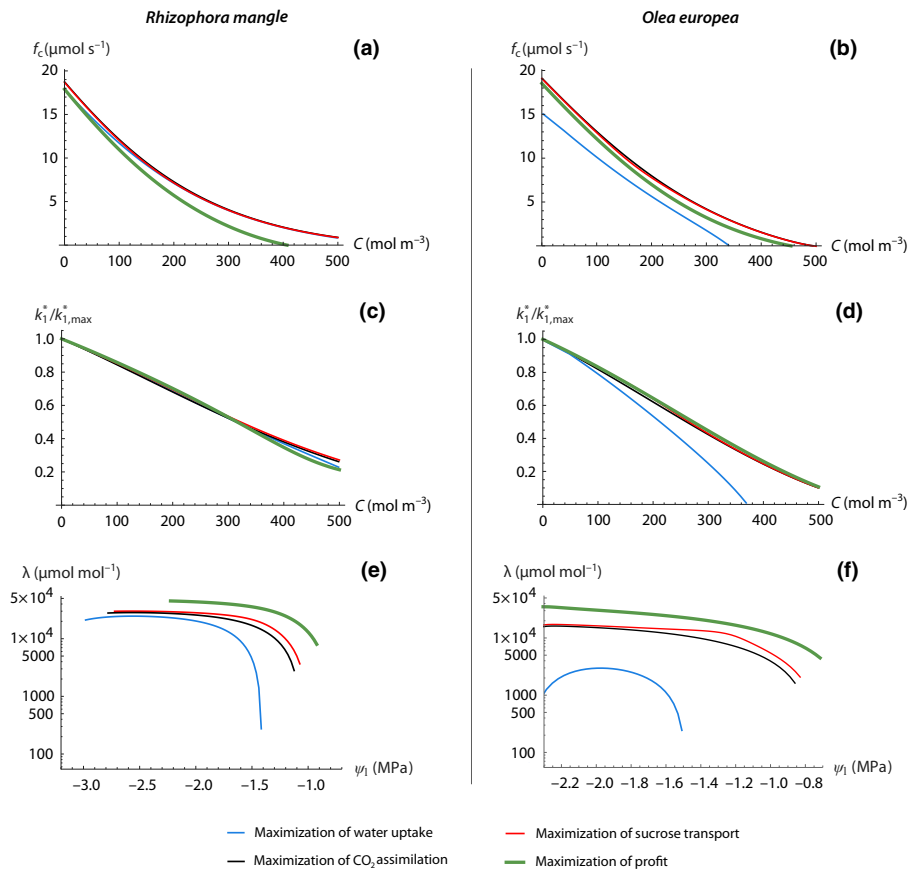
### Salinity impacts on CO<sub>2</sub> assimilation rate

Fig. 5(a,b) shows assimilation rate as a function of soil water salinity as obtained from Eqn 15 for the salt-tolerant and the salt-sensitive species. The assimilation rate does not

substantially change in *R. mangle* for the different optimality schemes (Eqn 15a–c) although the profit-maximization scheme results in a faster decay with increased salinity. *Olea europea* displays considerably lower  $f_c$  when the plant maximizes water uptake (blue curve in Fig. 5b). A possible explanation of this



**Fig. 4** (a, b) Transpiration rate  $T_r$  as a function of soil salinity  $C$  as obtained from the four optimality rules for *Rhizophora mangle* and *Olea europea*. (c–f) Comparison between modeled and observed relative transpiration rate  $T_r/T_{r,max}$  for (c) *R. mangle*, (d) *O. europea*, (e) *Avicennia marina*, and (f) *Plantago maritima* (data from Lin & da S. L. Sternberg, 1993; Ahmed *et al.*, 2008; Ball & Farquhar, 1984; Flanagan & Jefferies, 1989, respectively).



**Fig. 5** (a, b) Predicted CO<sub>2</sub> assimilation rate  $f_c$ , (c, d) relative apparent carboxylation rate  $k_1^*/k_{1,max}^*$ , and (e, f) marginal water use efficiency  $\lambda$  as a function of soil salinity  $C$  for *Rhizophora mangle* and *Olea europea*. The values of  $\psi_l$  are estimated through one of the four optimality rules: maximum water uptake (blue curves), maximum carbon assimilation (black curves), maximum sucrose transport (red curves) and maximum profit (dark green curves).

behavior is that the Eqn 15(a) leads to low  $\psi_l$  and elevated salt concentration in the leaf, which ultimately results in a partial or complete impairment of the carbon assimilation capability through reduced mesophyll conductance (see section ‘Reduction of apparent carboxylation capacity due to salt stress’). An increase in water uptake leads to higher salt uptake and salt stress.

**Reduction of apparent carboxylation capacity due to salt-stress** The biochemical parameters  $k_1$  and  $k_2$  in Eqn 7 are considered constant at the cell level and for sub-hourly timescales. However, the carboxylation capacity within the intercellular space ( $V_{c,max} = k_1^*$ ) is known to decrease during osmotic stress caused by droughts or salinity (Wang & Nii, 2000; Flexas & Medrano, 2002). To quantify the reduction  $k_1^*$  with increasing salinity, Eqn 7 describing the CO<sub>2</sub> demand at the cell level can be equated to:

$$f_{c,d}^* = \frac{k_1^*(c_i - \Gamma^*)}{k_2^* + c_i} - R_d. \quad \text{Eqn 16}$$

Then, coupling Eqns 16 to 9 and 8, an expression for  $k_1^*$  can be derived. This expression accounts for the reduction of the apparent maximum carboxylation rate due to salt stress. Fig. 5(c,d) shows the relative reduction of  $k_1^*$  as a function of  $C$ . The decline of  $k_1^*$  is congruent with plants maximizing carbon assimilation,

sucrose transport or carbon profit. To the contrary, the maximization of water uptake leads to larger reductions in apparent carboxylation rate, especially for *O. europea*. This finding is in agreement with observed inhibition of CO<sub>2</sub> fixation in glycophytes due to osmotic and ionic stress (Seemann & Critchley, 1985; Yeo *et al.*, 1991; Yensen & Biel, 2006; Stepien & Johnson, 2009).

**Marginal water use efficiency under salt stress** The flux-based water use efficiency is defined as  $WUE = f_c/f_e$  from which the marginal water use efficiency  $\lambda$  can be derived as (Hari *et al.*, 1986; Katul *et al.*, 2009; Manzoni *et al.*, 2011):

$$\lambda(\psi_l) = \frac{\partial f_c(\psi_l)/\partial g_s(\psi_l)}{\partial f_{e,s}(\psi_l)/\partial g_s(\psi_l)}. \quad \text{Eqn 17}$$

Marginal water use efficiency describes the cost of losing water in carbon units, thereby linking together the plant carbon and water economies. In water-stressed environments,  $\lambda(\psi_l)$  is expected to increase with decreasing  $\psi_l$  as the cost of losing water becomes higher with increased stress (Manzoni *et al.*, 2011, 2013a). Moreover, a nonconstant  $\lambda$  does not imply lack of optimal stomatal behavior (even in the SOT not accounting for salinity) but that the constraints are dictating the character of the optimal solution. Fig. 5(e,f) shows the modeled relation between  $\lambda$  and leaf water potential arising from all four optimization

schemes (Eqns 15a–d) for salt-tolerant (e) and sensitive plants (f). Notably, the concave downward pattern empirically observed by Manzoni *et al.* (2011) for drought experiments is recovered here from model calculations. The cost of losing water is generally higher in *R. mangle* than *O. europea*, with even larger costs in the case of profit-maximization. Elevated water uptake results in lower  $\lambda$ , especially for the salt-sensitive species.

## Sucrose transport

The effects of salinity on sucrose transport, which is rarely studied or reported in the literature, are shown in Fig. 6(a,b). The higher the salinity, the lower the transport of carbohydrates from the source to the sinks. Analogously to the assimilation rate,  $F_s$  is consistent among different maximization strategies in *R. mangle* with a faster decay under the profit-maximization scheme, whereas in *O. europea*  $f_{e,s}$  maximization causes a significant reduction in  $F_s$  production rate and transport. The advective component of sucrose transport ( $F_{s,adv} = C_s f_w$ ) can be dominant at high water potentials (i.e. for wet nonsaline soil), and it becomes negligible under severe salt stress when  $F_s$  is mainly osmotically driven. In *O. europea* the difference between advective and diffusive components is less marked than in *R. mangle*. Over a wide range of salinities, the two

components have a similar contribution to the sucrose movement. As a result, there is an inflection point in the  $F_s$  curve at intermediate salinity (Fig. 6b). The inflection is propagated to water and carbon fluxes in case of sucrose transport maximization.

The presence of inorganic ions ( $\text{Na}^+$  and  $\text{Cl}^-$ ) decreases the phloem osmotic potential and increases the driving force for sucrose movement. As shown in Fig. 6(c,d), the higher the salt concentration in the phloem, the larger the diffusive sucrose transport. This effect is particularly evident at high salinity, where the advective component of  $F_s$  is negligible, and the concentration of organic ions is low. The nonmonotonic pattern in the diffusive component of sucrose transport emerges as a result of changes in water viscosity described in the Materials and Methods section. As shown in Fig. 5(e,f), at low salinity elevated assimilation rate leads to high sucrose concentration in the phloem (i.e.  $C_{s,wt} \approx 60\%$  as sucrose weight fraction). Although the higher  $C_{s,wt}$  the larger the driving force, the presence of organic solutes increase sap viscosity drastically. As a consequence,  $F_{s,diff}$  becomes maximum at a well-defined optimal value of sucrose concentration ( $C_{s,wt} \approx 20\text{--}30\%$ ). This result is in agreement with measurements and previous estimations of optimal sucrose concentration in the phloem across a wide range of species (see Jensen *et al.*, 2013).

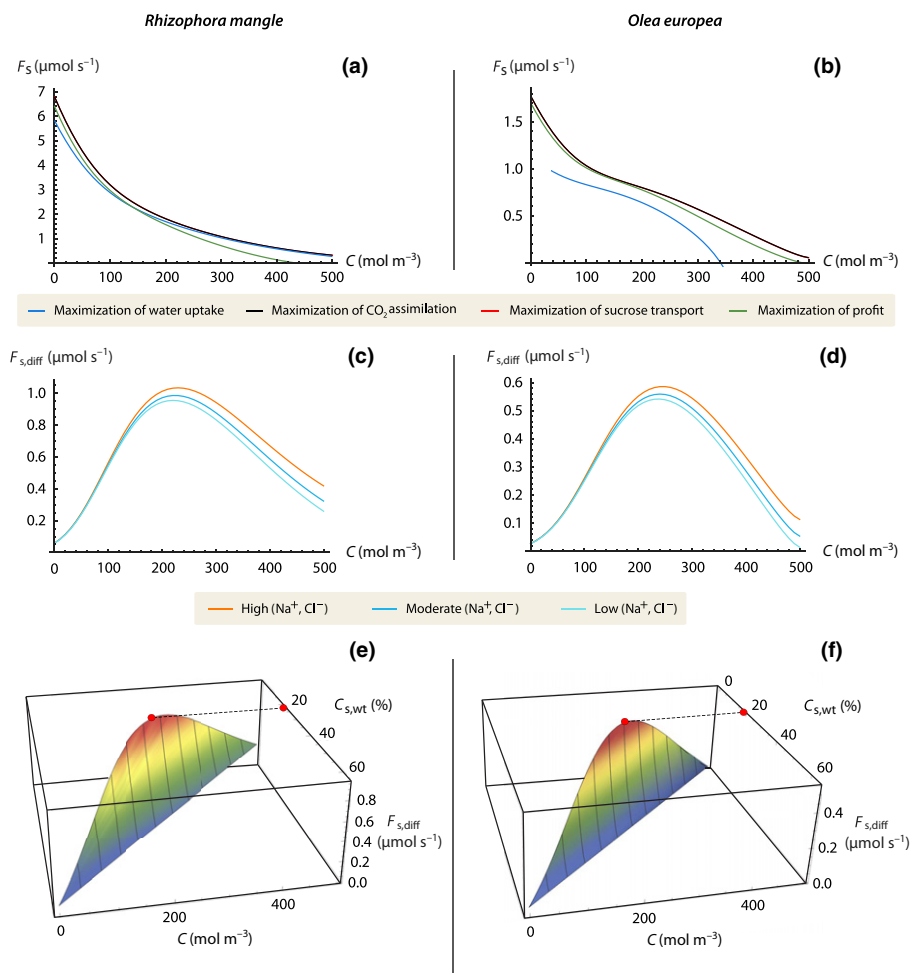


**Fig. 6** (a, b) Sucrose transport rate  $F_s$  as a function of salinity  $C$  for *Rhizophora mangle* and *Olea europea* as obtained from the four optimality rules. (c, d) Diffusive component of sucrose transport  $F_{s,diff}$  as a function of soil salinity for three different levels of salt concentration in the leaf-phloem: high ( $C_p = 250 \text{ mol m}^{-3}$ ; red curve), moderate ( $C_p = 150 \text{ mol m}^{-3}$ ; blue curve), and low ( $C_p = 50 \text{ mol m}^{-3}$ ; turquoise curve). (e, f) Diffusive sucrose transport as a function of salinity and carbohydrates concentration in the loading zone  $C_{s,wt}$ . It is worth noting that the optimal sucrose concentration corresponds to a value of approximately 20% (red dots), in agreement with an ensemble of experimental data reported by Jensen *et al.* (2016). The results in (c–e) are obtained according to the hypothesis expressed in Eqn 15(b).

## Model limitations

Here, a physically based but ‘zero-dimensional’ (i.e. no explicit spatial dimension considered) plant model is introduced to describe short-term effects of soil salinity on water, carbon and sucrose transport in plants. This minimalistic approach presents, however, a number of limitations. To start with, the focus was on quasi-instantaneous (i.e. sub-hourly) response of plants to salt exposure assuming steady-state conditions. This assumption is consistent with the observation that salt stress is dominated by the short and intense phase following the exposure (osmotic phase) whereas cytotoxic effects (ionic phase), and the subsequent morphological adaptations, can have a lower relative impact. At longer timescales, the transients in soil water balance and salt accumulation in plant tissues become major issues that must be resolved and cannot be captured by the assumed chemical equilibrium and membrane efficiency. Furthermore, fluctuating environmental conditions, especially incident radiation and air temperature, could affect stem water storage dynamics assumed to be constant here.

The zero-dimensionality also imposes limitations on how radiation transmission and aerodynamic effects due to wind–leaf interactions occur. For the same reason, nonlinear water–soil–root interactions are not included in this formulation. Processes such as hydraulic redistribution (i.e. passive water movement from wet to dry soil in the root zone; Scholz *et al.*, 2002; Moreira *et al.*, 2003; Domec *et al.*, 2004; Siqueira *et al.*, 2008; Huang *et al.*, 2017), and 3D gradients in soil moisture (Manoli *et al.*, 2014, 2017) and salinity that may impact the overall plant response to salt stress are not considered. The role of nutrient availability, which becomes essential to estimate biomass production, is not discussed here, being outside the present scope. Also, the lack of water, carbon and sucrose transport measurements under salt stress does not allow for a systematic model validation.

In spite of all these limitations, the proposed model represents a necessary first step to formulate a description of a coupled water, carbon and sucrose transport within the soil–plant system in saline environments. This formulation accommodates all the main processes that may be impacted by soil salinity and allows exploring various optimality rules required to mathematically ‘close’ the system and determine leaf water potential. Although a rigorous model validation cannot be performed, the approach can be used to interpret observed transpiration and photosynthesis patterns in halophytes and glycophytes. From this analysis, it is possible to formulate a number of hypotheses on the role of salinity on photosynthesis and plant–water relations and thus design future experiments to assess the model. Simultaneous measurements of gas exchange as a function of soil salinity as well as plant hydraulic traits and phloem properties are, clearly, urgently needed to further progress in the understanding of salt tolerance. In turn, sap flow data could be valuable as a proxy for transpiration and as a tool to capture the influence of transient dynamics on water movement within the plant.

By exploring only short-term salinity exposure, the proposed approach focuses on physiological mechanisms and allows us to momentarily neglect the morphological ones where acclimation

becomes necessary. Future work will consider soil–root and multi-canopy layers (Williams *et al.*, 1996; Siqueira *et al.*, 2008; Bonan *et al.*, 2014; García-Tejera *et al.*, 2017; Manoli *et al.*, 2017) as well as variable sources and sinks of sucrose along the phloem. A further extension of this model can account for dynamic soil water and salt mass balance (Daly *et al.*, 2004; Bartlett *et al.*, 2014; Hartzell *et al.*, 2018). Finally, nutrient limitations and plant–plant competition for light and water can be introduced through light attenuation, water budget and nutrients uptake schemes (Bohrer *et al.*, 2005; Šimůnek & Hopmans, 2009; Manzoni *et al.*, 2012; Manoli *et al.*, 2014, 2017; Huang *et al.*, 2018).

## Discussion

The plant conveyance systems are here parsimoniously represented, and all made to vary with leaf water potential. To determine the leaf water potential, an additional equation formulated as an optimality rule is introduced. Four plausible optimality rules are then explored and compared to determine  $\psi_l$  as a function of soil salinity. These rules require  $\psi_l$  to adjust so as to maximize  $f_{e,s}$ ,  $f_c$ ,  $F_s$  or  $G - \mathcal{R}$ . The same calculations subject to the same optimality rules are conducted for both salt-tolerant and salt-sensitive plants under well-watered conditions. Results from the three flux-maximization schemes (Eqns 15a–c) suggest that sucrose production and transport requires the largest leaf water potential and appears to be the dominant limitation. This result is reinforced for salt-sensitive species where maximization of water uptake significantly lowers  $\psi_l$  thereby limiting carbon assimilation and photosynthesis (see Figs 3–5). Interestingly, glycophytes are able to enhance water uptake above their physiological need to maintain optimal turgor.

In halophytes, the profit-maximization scheme has been shown to accentuate the adverse effects of cavitation with increasing salinity (Figs 3–6). By implicitly accounting for water competition, the hypothesis expressed in Eqn 15(d) may yield an evolutionarily stable strategy assuming that plants under stress mainly aim to save water (Wolf *et al.*, 2016; Sperry *et al.*, 2017). This hypothesis has found support in drought experiments (Anderegg *et al.*, 2018; Venturas *et al.*, 2018). However, in halophytes, the response to salt stress differs from the one to water stress, thereby leading to less conservative water use strategies (see section ‘Stress tolerance and mitigation’). Consequently, the definition of profit for salt-tolerant plants should include the effects of such adaptations and allow for distinguishing between hydraulic and salt-induced risk.

## Salinity controls on plant–water relations, water and carbon fluxes

Although the effect of salinity on xylem conductance is assumed similar for salt-tolerant and salt-sensitive species (Fig. 3c,d), the  $T_r - C$  patterns emerging from model calculations are different across species (Fig. 4). For glycophytes, the model reproduces a transpiration rate monotonically decreasing with increased soil salinity. To the contrary, a nonmonotonic  $T_r - C$  behavior has



been reported for several halophytes (Flowers *et al.*, 1977; Ball & Farquhar, 1984; Flanagan & Jefferies, 1989; Lin & da S. L. Sternberg, 1993; Becker *et al.*, 1997; Takemura *et al.*, 2000; Saenger, 2002) as a consequence of osmotic adjustment (Perri *et al.*, 2018a). Such nonmonotonic patterns are here recovered as a result of xylem–phloem interactions. The water/ions flux from the xylem to the phloem (and vice versa) supports optimal turgor pressure maintenance in saline conditions. However, at low salinity and elevated soil moisture, strongly negative internal water potential sustains a substantial osmoregulatory flux that limits transpiration. Elevated uptake of salt resulting from  $f_{e,s}$  maximization reduces mesophyll conductance to  $\text{CO}_2$  and abates the effective carboxylation rate. The introduction of  $g_m$  within the  $\text{CO}_2$  pathway accounts for such nonstomatal controls on carbon assimilation, which have been shown to be large in saline conditions (Volpe *et al.*, 2011). The decline in effective carboxylation rate (see Fig. 5c,d) is, therefore, a consequence of salt-induced mesophyll conductance reduction, ultimately affecting  $\text{CO}_2$  assimilation. By controlling  $f_{e,s}$  salinity has an appreciable impact on sucrose production (Eqn 13).

The effects of salinity on carbohydrate transport can be studied by investigating advective and diffusive components separately. In well-watered nonsaline soils, the advective component is larger than the diffusive one, and the opposite is observed at high salinity. The advective component monotonically decreases as a function of  $C$ , whereas the osmotically driven transport of sucrose presents a maximum at intermediate salinity (Fig. 6c,d). The latter is a consequence of the combined effect of the gradual increase in the driving force and the rapid increase in sap viscosity with sucrose concentration (that is maximum at high  $\psi_b$  Hölttä *et al.*, 2006, 2009; Jensen *et al.*, 2016; Konrad *et al.*, 2018).

When plants are able to use inorganic ions instead of photosynthetic products for osmotic adjustment, the energetic cost of salt tolerance is minimized (Arsova *et al.*, 2019). Osmoregulation

mechanisms allow salt-resilient plants to regulate internal water potential thorough ions (or water) movement across plant compartments more effectively than salt-sensitive species (Perri *et al.*, 2018a). The fact that the presence of a small amount of inorganic ions inside that plant can be beneficial for osmotic stress tolerance is also evident for sucrose transport, as discussed in section ‘Sucrose transport’. The higher the NaCl concentration in the phloem, the larger the driving force for diffusive transport (see Fig. 6c–f). As observed by Jensen *et al.* (2016) and Konrad *et al.* (2018), the presence of  $\text{Na}^+$  and  $\text{Cl}^-$  intensifies osmotic potential gradients without a significant increment in sap viscosity. High leaf salt concentration results in a ‘boost’ of  $F_{s,\text{diff}}$  directly proportional to the phloem osmotic potential due to inorganic ions ( $R i_v T_p C_p$ ). It is worth noting that elevated salt concentration in the leaf can cause ionic stress and can be maintained only if plants are able to avoid oxidative stress through ions compartmentalization (Binzel *et al.*, 1988; Parida & Das, 2005; Che-Othman *et al.*, 2019).

### Stress tolerance and mitigation

It is well-known that salt stress limits leaf gas exchanges by reducing stomatal conductance and apparent photosynthetic capacity (Munns & Gilliam, 2015). For this reason, salt and water stress may share similar adverse effects on plant–water relations (i.e. over the short-term they both cause osmotic stress; Lüttge, 1993; Munns, 2002). However, it is now accepted that plant response to salinity depends on adaptation mechanisms and can differ from water stress (Byrt & Munns, 2008; Munns & Tester, 2008). As shown in Fig. 7, the proposed framework accounts for these differing responses by estimating  $\psi_l$  as a function of soil water potential when this potential is changing due to  $C$  increment or  $s$  reduction. In *O. europea*, water and salt stress are shown to cause similar reductions in  $\psi_l$ . In *R. mangle*, leaf water

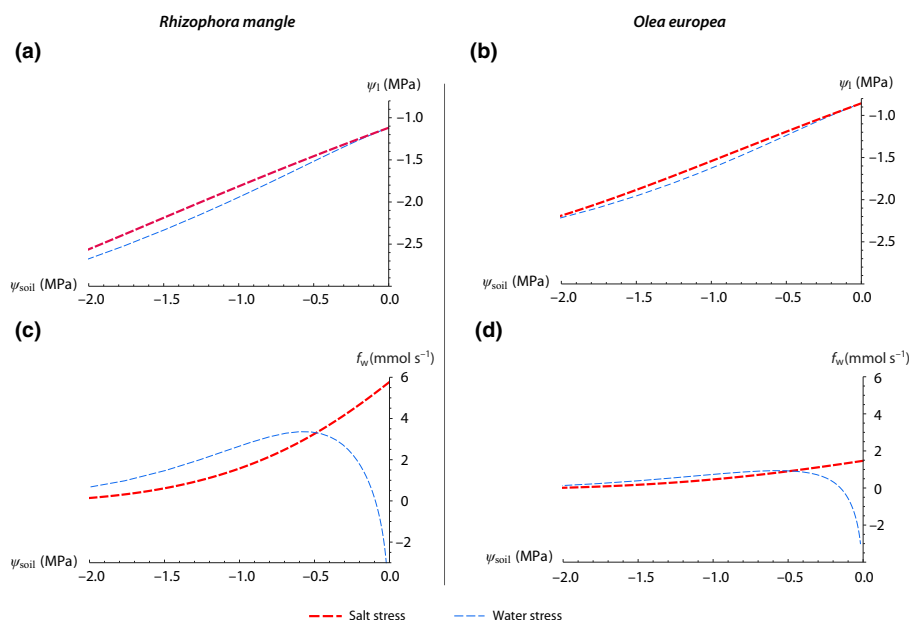


**Fig. 7** Comparison between leaf water potential  $\psi_l$  (a, b) and xylem–phloem water flux  $f_w$  (c, d) as a function of total soil water potential  $\psi_{\text{soil}}$  for water stress (dashed blue lines) and salt stress (dashed red lines) conditions. Water stress has been modeled using decreasing soil moisture and maintaining a null salt concentration. Salt stress is modeled by increasing salinity under well-watered soil conditions. Results are obtained according to the rule expressed in Eqn 15(b).

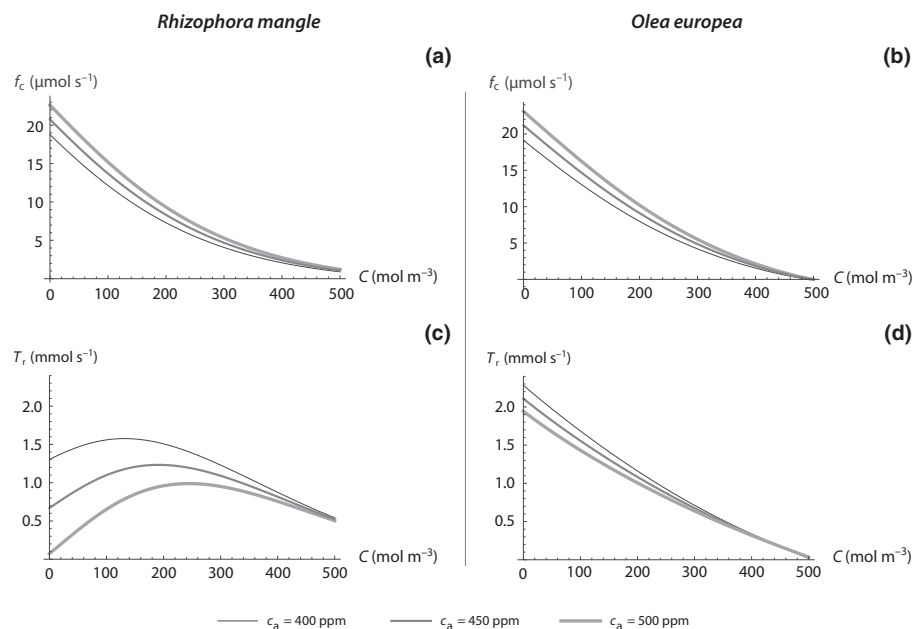


**Fig. 8** (a, b) Assimilation  $f_c$  and (c, d) transpiration rate  $T_r$  as a function of salinity  $C$  for three different levels of atmospheric  $\text{CO}_2$  concentration (400, 450 and 500 ppm). Results are obtained according to the hypothesis expressed in Eqn 15(b).

potential is lower under water stress than under salt stress for a given  $\psi_{\text{tot}}$ . Remarkably, this result reinforces experimental evidence that the effects of salt and water stress in salt-tolerant plants are neither identical nor cumulative (Richardson *et al.*, 1985; Omami & Hammes, 2006; Razzaghi *et al.*, 2011).

In *R. mangle*, the osmoregulatory flux ( $f_w$ ) significantly varies for water and salt stress (Fig. 7c). This explains the different controls exerted on leaf water potential by salt and drought. Salt-tolerant plants can then differentiate between salt- and drought-induced osmotic stress. By contrast, in *O. europaea*, osmoregulatory fluxes are considerably smaller (Fig. 7d), ultimately leading to water and salt stress having similar impacts on leaf water potential. Salt sensitivity emerges as a result of the incapability to distinguish between water and salt stress.

The ability to differentiate between water and salt stress is reflected in the diverse  $T_r - C$  patterns observed in experimental data and reproduced by the model (Fig. 4c–f). In particular, while glycophytes show a sharp decline in  $T_r$  as a function of  $C$  across all the maximization schemes, halophytes effectively maximize carbon assimilation (and sucrose transport) rather than water uptake or profit over the optimal salinity range.

Different strategies can be observed in woody (*R. mangle* and *A. marina*) and herbaceous (*P. maritima*) halophytes. It is reasonable to assume that the resilience of woody plants mainly relies on osmoregulation. As part of the osmoregulatory process, the production and dislocation of osmolytes is fundamental for the tolerance of moderate stress (Zimmermann *et al.*, 1994). As shown in the comparison between modeled and observed  $T_r - C$  patterns, woody halophytes are adapted to maximize growth up to an optimal intermediate salinity value ( $C_{\text{max}}$ ). For salinity larger than  $C_{\text{max}}$ , they have to adopt water-saving strategies to reduce the risk of cavitation. By contrast, herbaceous halophytes display lower vulnerability to cavitation and can tolerate lower water potentials. This allows herbaceous halophytes to maximize

growth (or photosynthesis here) over a wide range of salinity and to be less reliant on osmoregulation itself.

These results suggest that halophytes could be favored by future atmospheric fertilization through a *WUE* enhancement within their optimal range of salinity. The modeling framework proposed here allows to investigate this possible stress-mitigation effect. As shown in Fig. 8, an increment of  $c_a$  from 400 to 500 ppm results in larger assimilation rate and lower transpiration losses. This mitigation is only effective at low to moderate salinity but becomes negligible when approaching high salinity. *Rhizophora mangle* is substantially more sensitive to  $c_a$  variations than *O. europaea*. At low salinity, a small increment in  $c_a$  produces a large reduction in water losses in the salt-tolerant species, implying an increment in *WUE*. This result is in agreement with several experiments performed in controlled environments (Nicolas *et al.*, 1993; Geissler *et al.*, 2008, 2009, 2015; Melgar *et al.*, 2008; Mateos-Naranjo *et al.*, 2010; Pérez-Romero *et al.*, 2018, 2019). Moreover, the value of  $C$  at which  $T_r$  is maximum shifts to higher  $C$  values with increasing  $c_a$ . From an ecological perspective, this finding indicates that  $\text{C}_3$  halophytes could be favored by elevated  $\text{CO}_2$  conditions when competing with  $\text{C}_3$  glycophytes (McKee *et al.*, 2012).

Protracted exposure to atmospheric  $\text{CO}_2$  enrichment leads to morphological adaptations such as decrease in stomatal density (Woodward & Bazzaz, 1988; Pritchard *et al.*, 1998; Domec *et al.*, 2017). Similar adaptations are observed in halophytes thriving in saline environments (Poljakoff-Mayber, 1975; Xu *et al.*, 2016). Although morphological adaptations are not explicitly considered here, model results suggest that halophytes already possess the needed genetic machinery to implement these strategies, and could be favored by future  $\text{CO}_2$  fertilization. Although direct testing for these findings awaits field experiments, the work here does offer hypotheses and a list of variables that need to be measured to test them.




## Acknowledgements

This study was supported by Abu Dhabi Department of Education and Knowledge (ADEK), through project AARE17-250. GK acknowledges support from the US National Science Foundation (NSF-EAR-1344703, NSF-AGS-1644382 and NSF-IOS-1754893).

## Author contributions

SP, GGK and AM designed the model, its parameterization and the meta-analysis. SP led the model theory development and the meta-analysis, with the support of AM and GK. All authors contributed to writing the manuscript.

## ORCID

Gabriel G. Katul  <https://orcid.org/0000-0001-9768-3693>  
Annalisa Molini  <https://orcid.org/0000-0003-3815-3929>  
Saverio Perri  <https://orcid.org/0000-0001-6382-1381>

## References

- Ahmed CB, Rouina BB, Boukhris M. 2008. Changes in water relations, photosynthetic activity and proline accumulation in one-year-old olive trees (*Olea europaea* L. cv. *Chemlali*) in response to NaCl salinity. *Acta Physiologiae Plantarum* 30: 553–560.
- Alongi DM. 1998. *Coastal ecosystem processes*. Boca Raton, FL, USA: CRC Press.
- Ammari TG, Tahboub AB, Saoub HM, Hattar BI, Al-Zubi YA. 2008. Salt removal efficiency as influenced by phytoamelioration of salt-affected soils. *Journal of Food, Agriculture and Environment* 6: 456–460.
- Anderegg WR, Wolf A, Arango-Velez A, Choat B, Chmura DJ, Jansen S, Kolb T, Li S, Meinzer F, Pita P *et al.* 2017. Plant water potential improves prediction of empirical stomatal models. *PLoS ONE* 12: e0185481.
- Anderegg WR, Wolf A, Arango-Velez A, Choat B, Chmura DJ, Jansen S, Kolb T, Li S, Meinzer FC, Pita P *et al.* 2018. Woody plants optimise stomatal behaviour relative to hydraulic risk. *Ecology Letters* 21: 968–977.
- Arsova B, Foster KJ, Shelden MC, Bramley H, Watt M. 2019. Dynamics in plant roots and shoots minimise stress, save energy and maintain water and nutrient uptake. *New Phytologist*. doi: 10.1111/nph.15955.
- Ball MC, Farquhar GD. 1984. Photosynthetic and stomatal responses of two mangrove species, *Aegiceras corniculatum* and *Avicennia marina*, to long term salinity and humidity conditions. *Plant Physiology* 74: 1–6.
- Barr J. 2005. *Carbon sequestration by riverine mangroves in the Florida Everglades*. PhD thesis. University of Virginia, Charlottesville, VA, USA.
- Barr JG, Fuentes JD, Engel V, Zieman JC. 2009. Physiological responses of red mangroves to the climate in the Florida Everglades. *Journal of Geophysical Research: Biogeosciences* 114: G02008.
- Bartlett MS, Vico G, Porporato A. 2014. Coupled carbon and water fluxes in CAM photosynthesis: modeling quantification of water use efficiency and productivity. *Plant and Soil* 383: 111–138.
- Becker P, Asmat A, Mohamad J, Moksin M, Tyree MT. 1997. Sap flow rates of mangrove trees are not unusually low. *Trees, Structure and Function* 11: 432–435.
- Begg JE, Turner NC. 1976. Crop water deficits. *Advances in Agronomy* 28: 161–217.
- Binzel ML, Hess DF, Bressan RA, Hasegawa PM. 1988. Intracellular compartmentation of ions in salt adapted tobacco cells. *Plant Physiology* 86: 607–614.
- Bohrer G, Mourad H, Laursen TA, Drewry D, Avissar R, Poggi D, Oren R, Katul GG. 2005. Finite element tree crown hydrodynamics model (FETCH) using porous media flow within branching elements: a new representation of tree hydrodynamics. *Water Resources Research* 41: W11404.
- Bonan GB, Williams M, Fisher RA, Oleson KW. 2014. Modeling stomatal conductance in the earth system: linking leaf water-use efficiency and water transport along the soil-plant-atmosphere continuum. *Geoscientific Model Development* 7: 2193–2222.
- Bongi G, Loreto F. 1989. Gas-exchange properties of salt-stressed olive (*Olea europaea* L.) leaves. *Plant Physiology* 90: 1408–1416.
- Boyko H, Boyko E. 1959. Seawater irrigation a new line of research on a bioclimatic plant-soil complex. *International Journal of Bioclimatology and Biometeorology* 3: 33–61.
- Brugnoli E, Lauteri M. 1991. Effects of salinity on stomatal conductance, photosynthetic capacity, and carbon isotope discrimination of salt-tolerant (*Gossypium-hirsutum* L.) and salt-sensitive (*Phaseolus-vulgaris* L.) C<sub>3</sub> non-halophytes. *Plant Physiology* 95: 628–635.
- Buckingham E. 1907. *Studies on the movement of soil moisture, vol. 38*. Washington, DC, USA: USDA, Bureau of Soils.
- Buckley TN, Sack L, Farquhar GD. 2017. Optimal plant water economy. *Plant, Cell & Environment* 40: 881–896.
- Bui EN. 2013. Soil salinity: a neglected factor in plant ecology and biogeography. *Journal of Arid Environments* 92: 14–25.
- Byrt CS, Munns R. 2008. Living with salinity. *New Phytologist* 179: 903–905.
- Cannell MG, Thornley JH. 2000. Modelling the components of plant respiration: some guiding principles. *Annals of Botany* 85: 45–54.
- Casagrande E, Mueller B, Miralles DG, Entekhabi D, Molini A. 2015. Wavelet correlations to reveal multiscale coupling in geophysical systems. *Journal of Geophysical Research – Atmospheres* 120: 7555–7572.
- Chartzoulakis K, Loupassaki M, Bertaki M, Androulakis I. 2002. Effects of NaCl salinity on growth, ion content and CO<sub>2</sub> assimilation rate of six olive cultivars. *Scientia Horticulturae* 96: 235–247.
- Chaves M. 1991. Effects of water deficits on carbon assimilation. *Journal of Experimental Botany* 42: 1–16.
- Che-Othman MH, Jacoby RP, Millar AH, Taylor NL. 2019. Wheat mitochondrial respiration shifts from the tricarboxylic acid cycle to the GABA shunt under salt stress. *New Phytologist*. doi: 10.1111/nph.15713.
- Clapp RB, Hornberger GM. 1978. Empirical equations for some soil hydraulic properties. *Water Resources Research* 14: 601–604.
- Cochard H. 2006. Cavitation in trees. *Comptes Rendus Physique* 7: 1018–1026.
- Collatz GJ, Ball JT, Grivet C, Berry JA. 1991. Physiological and environmental regulation of stomatal conductance, photosynthesis and transpiration: a model that includes a laminar boundary layer. *Agricultural & Forest Meteorology* 54: 107–136.
- Comstock JP, Sperry JS. 2000. Theoretical considerations of optimal conduit length for water transport in vascular plants. *New Phytologist* 148: 195–218.
- Cowan IR. 1982. Regulation of water use in relation to carbon gain in higher plants. In: Lange OL, Nobel PS, Osmond CB, Ziegler H, eds. *Physiological plant ecology II*. Berlin, Germany: Springer, 589–613.
- Cowan IR, Farquhar GD. 1977. Stomatal function in relation to leaf metabolism and environment. *Symposia of the Society for Experimental Biology* 31: 471–505.
- Daly E, Porporato A, Rodriguez-Iturbe I. 2004. Coupled dynamics of photosynthesis, transpiration, and soil water balance. Part I: upscaling from hourly to daily level. *Journal of Hydrometeorology* 5: 546–558.
- Damour G, Simonneau T, Cochard H, Urban L. 2010. An overview of models of stomatal conductance at the leaf level. *Plant, Cell & Environment* 33: 1419–1438.
- Daneshmand H, Alaghmand S, Camporese M, Talei A, Daly E. 2019. Water and salt balance modelling of intermittent catchments using a physically-based integrated model. *Journal of Hydrology* 568: 1017–1030.
- Datta KK, Jong CD. 2002. Adverse effect of water logging and soil salinity on crop and land productivity in northwest region of Haryana, India. *Agricultural Water Management* 57: 223–238.
- Delfine S, Alvino A, Villani MC, Loreto F. 1999. Restrictions to carbon dioxide conductance and photosynthesis in spinach leaves recovering from salt stress. *Plant Physiology* 119: 1101–1106.
- Delfine S, Alvino A, Zacchini M, Loreto F. 1998. Consequences of salt stress on conductance to CO<sub>2</sub> diffusion, Rubisco characteristics and anatomy of spinach leaves. *Australian Journal of Plant Physiology* 25: 395–402.



- Dewar R, Mauranen A, Mäkelä A, Hölttä T, Medlyn B, Vesala T. 2018. New insights into the covariation of stomatal, mesophyll and hydraulic conductances from optimization models incorporating nonstomatal limitations to photosynthesis. *New Phytologist* 217: 571–585.
- Dingman SL. 2015. *Physical hydrology*. New York, NY, USA: Macmillan.
- Domec JC, Smith DD, McCulloh KA. 2017. A synthesis of the effects of atmospheric carbon dioxide enrichment on plant hydraulics: implications for whole-plant water use efficiency and resistance to drought. *Plant, Cell & Environment* 40: 921–937.
- Domec JC, Warren JM, Meinzer FC, Brooks JR, Coulombe R. 2004. Native root xylem embolism and stomatal closure in stands of douglas-fir and ponderosa pine: mitigation by hydraulic redistribution. *Oecologia* 141: 7–16.
- Eller CB, Rowland L, Oliveira RS, Bittencourt PR, Barros FV, da Costa AC, Meir P, Friend AD, Mencuccini M, Sitch S *et al.* 2018. Modelling tropical forest responses to drought and El Niño with a stomatal optimization model based on xylem hydraulics. *Philosophical Transactions of the Royal Society of London. Series B, Biological sciences* 373: 20170315.
- Epstein E, Norlyn JD, Rush DW, Kingsbury RW, Kelley DB, Cunningham GA, Wrona AF. 1980. Saline culture of crops: a genetic approach. *Science* 210: 399–404.
- FAO. 2015. Status of the World's Soil Resources (SWSR). *Tech. rep.* Rome, Italy: FAO.
- Farquhar GD, von Caemmerer S, Berry JA. 1980. A biochemical model of photosynthetic CO<sub>2</sub> assimilation in leaves of C<sub>3</sub> species. *Planta* 149: 78–90.
- Fatichi S, Leuzinger S, Paschalis A, Langley JA, Donnellan Barraclough A, Hovenden MJ. 2016. Partitioning direct and indirect effects reveals the response of water-limited ecosystems to elevated CO<sub>2</sub>. *Proceedings of the National Academy of Sciences, USA* 113: 12757–12762.
- Fatichi S, Pappas C, Zscheischler J, Leuzinger S. 2019. Modelling carbon sources and sinks in terrestrial vegetation. *New Phytologist* 221: 652–668.
- Flanagan L, Jefferies R. 1989. Photosynthetic and stomatal responses of the halophyte, *Plantago maritima* L. to fluctuations in salinity. *Plant, Cell & Environment* 12: 559–568.
- Flexas J, Bota J, Loreto F, Cornic G, Sharkey TD. 2004. Diffusive and metabolic limitations to photosynthesis under drought and salinity in C<sub>3</sub> plants. *Plant Biology* 6: 269–279.
- Flexas J, Medrano H. 2002. Drought-inhibition of photosynthesis in C<sub>3</sub> plants: stomatal and non-stomatal limitations revisited. *Annals of Botany* 89: 183–189.
- Flowers TJ, Troke PF, Yeo AR. 1977. The mechanism of salt tolerance in halophytes. *Annual Review of Plant Physiology* 28: 89–121.
- García-Legaz MF, Ortiz JM, García-Lidón A, Cerdá A. 1993. Effect of salinity on growth, ion content and CO<sub>2</sub> assimilation rate in lemon varieties on different rootstocks. *Physiologia Plantarum* 89: 427–432.
- García-Tejera O, López-Bernal Á, Testi L, Villalobos FJ. 2017. A soil-plant-atmosphere continuum (SPAC) model for simulating tree transpiration with a soil multi-compartment solution. *Plant and Soil* 412: 215–233.
- Geissler N, Hussin S, El-Far MM, Koyro HW. 2015. Elevated atmospheric CO<sub>2</sub> concentration leads to different salt resistance mechanisms in a C<sub>3</sub> (*Chenopodium quinoa*) and a C<sub>4</sub> (*Atriplex nummularia*) halophyte. *Environmental and Experimental Botany* 118: 67–77.
- Geissler N, Hussin S, Koyro HW. 2008. Elevated atmospheric CO<sub>2</sub> concentration ameliorates effects of NaCl salinity on photosynthesis and leaf structure of *Aster tripolium* L. *Journal of Experimental Botany* 60: 137–151.
- Geissler N, Hussin S, Koyro HW. 2009. Interactive effects of NaCl salinity and elevated atmospheric CO<sub>2</sub> concentration on growth, photosynthesis, water relations and chemical composition of the potential cash crop halophyte *Aster tripolium* L. *Environmental and Experimental Botany* 65: 220–231.
- Ghassemi F, Jakeman AJ, Nix HA. 1995. *Salinisation of land and water resources: human causes, extent, management and case studies*. Wallingford, UK: CAB International.
- Giaquinta RT. 1983. Phloem loading of sucrose. *Annual Review of Plant Biology* 34: 347–387.
- Glenn EP, Brown JJ, Blumwald E. 1999. Salt tolerance and crop potential of halophytes. *Critical Reviews in Plant Sciences* 18: 227–255.
- Gómez JA, Giráldez JV, Fereres E. 2001. Rainfall interception by olive trees in relation to leaf area. *Agricultural Water Management* 49: 65–76.
- Good SP, Moore GW, Miralles DG. 2017. A mesic maximum in biological water use demarcates biome sensitivity to aridity shifts. *Nature Ecology and Evolution* 1: 1883–1888.
- Haghighi M, Pesarakli M. 2013. Influence of silicon and nano-silicon on salinity tolerance of cherry tomatoes (*Solanum lycopersicum* L.) at early growth stage. *Scientia Horticulturae* 161: 111–117.
- Hari P, Mäkelä A, Korpilahti E, Holmberg M. 1986. Optimal control of gas exchange. *Tree Physiology* 2: 169–175.
- Hartzell S, Bartlett MS, Porporato A. 2018. Unified representation of the C<sub>3</sub>, C<sub>4</sub>, and CAM photosynthetic pathways with the Photo3 model. *Ecological Modelling* 384: 173–187.
- Herbert ER, Boon P, Burgin AJ, Neubauer SC, Franklin RB, Ardón M, Hopfensperger KN, Lamers LPM, Gell P. 2015. A global perspective on wetland salinization: ecological consequences of a growing threat to freshwater wetlands. *Ecosphere* 6: 1–43.
- Hirschi M, Seneviratne SI, Alexandrov V, Boberg F, Boroneant C, Christensen OB, Formayer H, Orlowsky B, Stepanek P. 2011. Observational evidence for soil-moisture impact on hot extremes in southeastern Europe. *Nature Geoscience* 4: 17–21.
- Hölttä T, Lintunen A, Chan T, Mäkelä A, Nikinmaa E. 2017. A steady-state stomatal model of balanced leaf gas exchange, hydraulics and maximal source-sink flux. *Tree Physiology* 37: 851–868.
- Hölttä T, Mencuccini M, Nikinmaa E. 2009. Linking phloem function to structure: analysis with a coupled xylem-phloem transport model. *Journal of Theoretical Biology* 259: 325–337.
- Hölttä T, Vesala T, Sevanto S, Perämäki M, Nikinmaa E. 2006. Modeling xylem and phloem water flows in trees according to cohesion theory and Münch hypothesis. *Trees-Structure and Function* 20: 67–78.
- Huang C-W, Domec J-C, Palmroth S, Pockman WT, Litvak ME, Katul GG. 2018. Transport in a coordinated soil root-xylem-phloem leaf system. *Advances in Water Resources* 119: 1–16.
- Huang C-W, Domec J-C, Ward EJ, Duman T, Manoli G, Parolari AJ, Katul GG. 2017. The effect of plant water storage on water fluxes within the coupled soil-plant system. *New Phytologist* 213: 1093–1106.
- Jensen KH, Berg-Sørensen K, Bruus H, Holbrook NM, Liesche J, Schulz A, Zwieniecki MA, Bohr T. 2016. Sap flow and sugar transport in plants. *Reviews of Modern Physics* 88: 035007.
- Jensen KH, Savage JA, Holbrook NM. 2013. Optimal concentration for sugar transport in plants. *Journal of the Royal Society, Interface* 10: 20130055.
- Jesus JM, Danko AS, Fiúza A, Borges M-T. 2015. Phytoremediation of salt-affected soils: a review of processes, applicability, and the impact of climate change. *Environmental Science and Pollution Research International* 22: 6511–6525.
- Jobbágy EG, Jackson RB. 2004. Groundwater use and salinization with grassland afforestation. *Global Change Biology* 10: 1299–1312.
- Kathilankal JC, Mozdzer TJ, Fuentes JD, D'Odorico P, McGlathery KJ, Zieman JC. 2008. Tidal influences on carbon assimilation by a salt marsh. *Environmental Research Letters* 3: 044010.
- Katul GG, Manzoni S, Palmroth S, Oren R. 2010. A stomatal optimization theory to describe the effects of atmospheric CO<sub>2</sub> on leaf photosynthesis and transpiration. *Annals of Botany* 105: 431–442.
- Katul GG, Palmroth S, Oren R. 2009. Leaf stomatal responses to vapour pressure deficit under current and CO<sub>2</sub>-enriched atmosphere explained by the economics of gas exchange. *Plant, Cell & Environment* 32: 968–979.
- Khan MA, Ungar IA, Showalter AM. 2000. Effects of salinity on growth, water relations and ion accumulation of the subtropical perennial halophyte, *Atriplex griffithii* var. *stocksii*. *Annals of Botany* 85: 225–232.
- Kirwan ML, Guntenspergen GR, D'Alpaos A, Morris JT, Mudd SM, Temmerman S. 2010. Limits on the adaptability of coastal marshes to rising sea level. *Geophysical Research Letters* 37: L23401.
- Konrad W, Katul GG, Roth-Nebelsick A, Jensen KH. 2018. Xylem functioning, dysfunction and repair: a physical perspective and implications for phloem transport. *Tree Physiology* 154: 1088–1107.
- Kumar KN, Molini A, Ouarda TB, Rajeevan MN. 2017. North Atlantic controls on wintertime warm extremes and aridification trends in the Middle East. *Scientific Reports* 7: 12301.



- Lampinen MJ, Noponen T. 2003. Thermodynamic analysis of the interaction of the xylem water and phloem sugar solution and its significance for the cohesion theory. *Journal of Theoretical Biology* 224: 285–298.
- Langley JA, Magonigal JP. 2010. Ecosystem response to elevated CO<sub>2</sub> levels limited by nitrogen-induced plant species shift. *Nature* 466: 96–99.
- Lin G, da S. L. Sternberg L. 1993. Effects of salinity fluctuation on photosynthetic gas exchange and plant growth of the red mangrove (*Rhizophora mangle* L.). *Journal of Experimental Botany* 44: 9–16.
- Lombardini L. 2006. Ecophysiology of plants in dry environments. In: D'Odorico P, Porporato A, eds. *Dryland ecohydrology*. Dordrecht, the Netherlands: Springer, 47–65.
- Longstreth DJ, Nobel PS. 1979. Salinity effects on leaf anatomy: consequences for photosynthesis. *Plant Physiology* 63: 700–703.
- Love D, Venturas M, Sperry J, Brooks P, Pettit J, Wang Y, Anderegg W, Tai X, Mackay D. 2019. Dependence of aspen stands on a subsurface water subsidy: implications for climate change impacts. *Water Resources Research* 55: 1833–1848.
- Lüttge U. 1993. The role of crassulacean acid metabolism (CAM) in the adaptation of plants to salinity. *New Phytologist* 125: 59–71.
- Manoli G, Bonetti S, Domec JC, Putti M, Katul GG, Marani M. 2014. Tree root systems competing for soil moisture in a 3D soil-plant model. *Advances in Water Resources* 66: 32–42.
- Manoli G, Huang CW, Bonetti S, Domec JC, Marani M, Katul GG. 2017. Competition for light and water in a coupled soil-plant system. *Advances in Water Resources* 108: 216–230.
- Manzoni S, Taylor P, Richter A, Porporato A, Ågren GI. 2012. Environmental and stoichiometric controls on microbial carbon-use efficiency in soils. *New Phytologist* 196: 79–91.
- Manzoni S, Vico G, Katul GG, Fay PA, Polley W, Palmroth S, Porporato A. 2011. Optimizing stomatal conductance for maximum carbon gain under water stress: a meta-analysis across plant functional types and climates. *Functional Ecology* 25: 456–467.
- Manzoni S, Vico G, Palmroth S, Porporato A, Katul G. 2013a. Optimization of stomatal conductance for maximum carbon gain under dynamic soil moisture. *Advances in Water Resources* 62: 90–105.
- Manzoni S, Vico G, Porporato A, Katul GG. 2013b. Biological constraints on water transport in the soil-plant atmosphere system. *Advances in Water Resources* 51: 292–304.
- Marchesini VA, Giménez R, Nasetto MD, Jobbágy EG. 2017. Ecohydrological transformation in the Dry Chaco and the risk of dryland salinity: following Australia's footsteps? *Ecohydrology* 10: e1822.
- Mateos-Naranjo E, Redondo-Gómez S, Álvarez R, Cambrollé J, Gandullo J, Figueroa ME. 2010. Synergic effect of salinity and CO<sub>2</sub> enrichment on growth and photosynthetic responses of the invasive cord grass *Spartina densiflora*. *Journal of Experimental Botany* 61: 1643–1654.
- McKee K, Rogers K, Saintilan N. 2012. Response of salt marsh and mangrove wetlands to changes in atmospheric CO<sub>2</sub>, climate, and sea level. In: Middleton BA, ed. *Global change and the function and distribution of wetlands*. Berlin, Germany: Springer, 63–96.
- Medlyn BE, Dreyer E, Ellsworth D, Forstreuter M, Harley PC, Kirschbaum MU, Le Roux X, Montpied P, Strassmeyer J, Walcroft A *et al.* 2002. Temperature response of parameters of a biochemically based model of photosynthesis. II. A review of experimental data. *Plant, Cell & Environment* 25: 1167–1179.
- Medlyn BE, Duursma RA, Eamus D, Ellsworth DS, Prentice IC, Barton CV, Crous KY, De Angelis P, Freeman M, Wingate L. 2011. Reconciling the optimal and empirical approaches to modelling stomatal conductance. *Global Change Biology* 17: 2134–2144.
- Meinzer FC, Grantz DA. 1990. Stomatal and hydraulic conductance in growing sugarcane: stomatal adjustment to water transport capacity. *Plant, Cell & Environment* 13: 383–388.
- Meinzer FC, Johnson DM, Lachenbruch B, McCulloh KA, Woodruff DR. 2009. Xylem hydraulic safety margins in woody plants: coordination of stomatal control of xylem tension with hydraulic capacitance. *Functional Ecology* 23: 922–930.
- Melgar JC, Syvertsen JP, García-Sánchez F. 2008. Can elevated CO<sub>2</sub> improve salt tolerance in olive trees? *Journal of Plant Physiology* 165: 631–640.
- Mencuccini M, Hölttä T. 2010. The significance of phloem transport for the speed with which canopy photosynthesis and belowground respiration are linked. *New Phytologist* 185: 189–203.
- Mencuccini M, Manzoni S, Christoffersen B. 2019. Modelling water fluxes in plants: from tissues to biosphere. *New Phytologist* 222: 1207–1222.
- Miralles DG, Van Den Berg MJ, Teuling AJ, De Jeu RAM. 2012. Soil moisture-temperature coupling: a multiscale observational analysis. *Geophysical Research Letters* 39: L21707.
- Moreira MZ, Scholz FG, Bucci SJ, Sternberg LS, Goldstein G, Meinzer FC, Franco AC. 2003. Hydraulic lift in a neotropical savanna. *Functional Ecology* 17: 573–581.
- Morgan JM. 1984. Osmoregulation and water-stress in higher-plants. *Annual Review of Plant Physiology* 35: 299–319.
- Munns R. 2002. Comparative physiology of salt and water stress. *Plant, Cell & Environment* 25: 239–250.
- Munns R, Gilliam M. 2015. Salinity tolerance of crops – what is the cost? *New Phytologist* 208: 668–673.
- Munns R, Termaat A. 1986. Whole-plant responses to salinity. *Australian Journal of Plant Physiology* 13: 143–160.
- Munns R, Tester M. 2008. Mechanisms of salinity tolerance. *Annual Review of Plant Biology* 59: 651–681.
- Negrão S, Schmöckel SM, Tester M. 2017. Evaluating physiological responses of plants to salinity stress. *Annals of Botany* 119: 1–11.
- Nicolas M, Munns R, Samarakoon A, Gifford R. 1993. Elevated CO<sub>2</sub> improves the growth of wheat under salinity. *Australian Journal of Plant Physiology* 20: 349–360.
- Nikinmaa E, Hölttä T, Hari P, Kolari P, Mäkelä A, Savanto S, Vesala T. 2013. Assimilate transport in phloem sets conditions for leaf gas exchange. *Plant, Cell & Environment* 36: 655–669.
- Nikinmaa E, Sievänen R, Hölttä T. 2014. Dynamics of leaf gas exchange, xylem and phloem transport, water potential and carbohydrate concentration in a realistic 3-D model tree crown. *Annals of Botany* 114: 653–666.
- Nobel PS. 1983. *Biophysical plant physiology and ecology*. San Francisco, CA, USA: WH Freeman.
- Novick KA, Miniat CF, Vose JM. 2016. Drought limitations to leaf-level gas exchange: results from a model linking stomatal optimization and cohesion-tension theory. *Plant, Cell & Environment* 39: 583–596.
- Oldeman L, Hakkeling RTA, Sombroek WG. 1990. *World map of the status of human-induced soil degradation: an explanatory note*. Wageningen, the Netherlands: ISRIC.
- Omami EN, Hammes PS. 2006. Interactive effects of salinity and water stress on growth, leaf water relations, and gas exchange in amaranth (*Amaranthus* spp.). *New Zealand Journal of Crop and Horticultural Science* 34: 33–44.
- Pankova YI, Konyushkova MV. 2014. Effect of global warming on soil salinity of the arid regions. *Russian Agricultural Sciences* 39: 464–467.
- Parida AK, Das AB. 2005. Salt tolerance and salinity effects on plants: a review. *Ecotoxicology and Environmental Safety* 60: 324–349.
- Parida AK, Jha B. 2010. Salt tolerance mechanisms in mangroves: a review. *Trees-Structure and Function* 24: 199–217.
- Paschalis A, Katul GG, Fatichi S, Palmroth S, Way D. 2017. On the variability of the ecosystem response to elevated atmospheric CO<sub>2</sub> across spatial and temporal scales at the Duke Forest FACE experiment. *Agricultural & Forest Meteorology* 232: 367–383.
- Passioura JB, Ball MC, Knight JH. 1992. Mangroves may salinize the soil and in so doing limit their transpiration rate. *Functional Ecology* 6: 476–481.
- Pérez-Romero JA, Duarte B, Barcia-Piedras J-M, Matos AR, Redondo-Gómez S, Caçador I, Mateos-Naranjo E. 2019. Investigating the physiological mechanisms underlying *Salicornia ramosissima* response to atmospheric CO<sub>2</sub> enrichment under coexistence of prolonged soil flooding and saline excess. *Plant Physiology and Biochemistry* 135: 149–159.
- Pérez-Romero JA, Idaszkin YL, Barcia-Piedras JM, Duarte B, Redondo-Gómez S, Caçador I, Mateos-Naranjo E. 2018. Disentangling the effect of atmospheric CO<sub>2</sub> enrichment on the halophyte *Salicornia ramosissima* J. Woods physiological performance under optimal and suboptimal saline conditions. *Plant Physiology and Biochemistry* 127: 617–629.

- Perri S, Entekhabi D, Molini A. 2018a. Plant osmoregulation as an emergent water-saving adaptation. *Water Resources Research* 54: 2781–2798.
- Perri S, Suweis S, Entekhabi D, Molini A. 2018b. Vegetation controls on dryland salinity. *Geophysical Research Letters* 45: 669–682.
- Perri S, Viola F, Noto LV, Molini A. 2017. Salinity and periodic inundation controls on the soil-plant-atmosphere continuum of gray mangroves. *Hydrological Processes* 31: 1271–1282.
- Pickard WF. 1981. The ascent of sap in plants. *Progress in Biophysics and Molecular Biology* 37: 181–229.
- Pitman MG, Läuchli A. 2002. Global impact of salinity and agricultural ecosystems. In: Läuchli A, Lüttge U, eds. *Salinity: environment-plants molecules*. Berlin, Germany: Springer, 3–20.
- Poljakoff-Mayber A. 1975. Morphological and anatomical changes in plants as a response to salinity stress. In: Poljakoff-Mayber A, Gale J, eds. *Plants in saline environments*. Berlin, Germany: Springer, 97–117.
- Pritchard SG, Mosjidic C, Peterson CM, Runion GB, Rogers HH. 1998. Anatomical and morphological alterations in longleaf pine needles resulting from growth in elevated CO<sub>2</sub>: interactions with soil resource availability. *International Journal of Plant Sciences* 159: 1002–1009.
- Qadir M, Ghafoor A, Murtaza G. 2000. Amelioration strategies for saline soils: a review. *Land Degradation & Development* 11: 501–521.
- Qadir M, Quillérrou E, Nangia V, Murtaza G, Singh M, Thomas RJ, Drechsel P, Noble AD. 2014. Economics of salt-induced land degradation and restoration. *Natural Resources Forum* 38: 282–295.
- Qadir M, Qureshi RH, Ahmad N, Ilyas M. 1996. Salt-tolerant forage cultivation on a saline-sodic field for biomass production and soil reclamation. *Land Degradation & Development* 7: 11–18.
- Ranney TG, Whitlow TH, Bassuk NL. 1990. Response of five temperate deciduous tree species to water stress. *Tree Physiology* 6: 439–448.
- Razzaghi F, Ahmadi SH, Adolf VI, Jensen CR, Jacobsen SE, Andersen MN. 2011. Water relations and transpiration of quinoa (*Chenopodium quinoa* Willd.) under salinity and soil drying. *Journal of Agronomy and Crop Science* 197: 348–360.
- Razzaghi F, Jacobsen SE, Jensen CR, Andersen MN. 2015. Ionic and photosynthetic homeostasis in quinoa challenged by salinity and drought – mechanisms of tolerance. *Functional Plant Biology* 42: 136–148.
- Rennie EA, Turgeon R. 2009. A comprehensive picture of phloem loading strategies. *Proceedings of the National Academy of Sciences, USA* 106: 14162–14167.
- Richardson SG, McCree KJ. *et al.* 1985. Carbon balance and water relations of sorghum exposed to salt and water stress. *Plant Physiology* 79: 1015–1020.
- Riederer M, Muller C. 2008. *Biology of the plant cuticle*, vol. 23. Oxford, UK: Blackwell Publishing.
- Rohades J, Kandiah A, Mashali A. 1992. *The use of saline waters for crop production*, vol. 48. Rome, Italy: FAO Irrigation & Drainage Paper.
- Runyan CW, D'Odorico P. 2010. Ecohydrological feedbacks between salt accumulation and vegetation dynamics: role of vegetation-groundwater interactions. *Water Resources Research* 46: W11561.
- Saenger P. 2002. *Mangrove ecology, silviculture and conservation*. London, UK: Klumer Academic.
- Salleo S, Nardini A, Pitt F, LoGullo MA. 2000. Xylem cavitation and hydraulic control of stomatal conductance in laurel (*Laurus nobilis* L.). *Plant, Cell & Environment* 23: 71–79.
- Sánchez FJ, Manzanares M, De Andres EF, Tenorio JL, Ayerbe L. 1998. Turgor maintenance, osmotic adjustment and soluble sugar and proline accumulation in 49 pea cultivars in response to water stress. *Field Crops Research* 59: 225–235.
- Schofield RV, Kirkby MJ. 2003. Application of salinization indicators and initial development of potential global soil salinization scenario under climatic change. *Global Biogeochemical Cycles* 17: 1–13.
- Scholander P. 1968. How mangroves desalinate seawater. *Physiologia Plantarum* 21: 251–261.
- Scholander P, Bradstreet ED, Hammel H, Hemmingsen E. 1966. Sap concentrations in halophytes and some other plants. *Plant Physiology* 41: 529–532.
- Scholz FG, Bucci SJ, Goldstein G, Meinzer FC, Franco AC. 2002. Hydraulic redistribution of soil water by neotropical savanna trees. *Tree Physiology* 22: 603–612.
- Seemann JR, Critchley C. 1985. Effects of salt stress on the growth, ion content, stomatal behaviour and photosynthetic capacity of a salt-sensitive species, *Phaseolus vulgaris* L. *Planta* 164: 151–162.
- Šimunek J, Hopmans JW. 2009. Modeling compensated root water and nutrient uptake. *Ecological Modelling* 220: 505–521.
- Sinclair T, Murphy C, Knoerr K. 1976. Development and evaluation of simplified models for simulating canopy photosynthesis and transpiration. *Journal of Applied Ecology* 13: 813–829.
- Siqueira M, Katul GG, Porporato A. 2008. Onset of water stress, hysteresis in plant conductance, and hydraulic lift: scaling soil water dynamics from millimeters to meters. *Water Resources Research* 44: W01432.
- Sobrado MA. 2007. Relationship of water transport to anatomical features in the mangrove *Laguncularia racemosa* grown under contrasting salinities. *New Phytologist* 173: 584–591.
- Sperry JS. 2000. Hydraulic constraints on plant gas exchange. *Agricultural & Forest Meteorology* 104: 13–23.
- Sperry JS, Adler F, Campbell G, Comstock J. 1998. Limitation of plant water use by rhizosphere and xylem conductance: results from a model. *Plant, Cell & Environment* 21: 347–359.
- Sperry JS, Venturas MD, Anderegg WR, Mencuccini M, Mackay DS, Wang Y, Love DM. 2017. Predicting stomatal responses to the environment from the optimization of photosynthetic gain and hydraulic cost. *Plant, Cell & Environment* 40: 816–830.
- Sperry JS, Wang Y, Wolfe BT, Mackay DS, Anderegg WR, McDowell NG, Pockman WT. 2016. Pragmatic hydraulic theory predicts stomatal responses to climatic water deficits. *New Phytologist* 212: 577–589.
- Steduto P, Albrizio R, Giorio P, Sorrentino G. 2000. Gas-exchange response and stomatal and non-stomatal limitations to carbon assimilation of sunflower under salinity. *Environmental and Experimental Botany* 44: 243–255.
- Stepien P, Johnson GN. 2009. Contrasting responses of photosynthesis to salt stress in the glycophyte *Arabidopsis* and the halophyte *Thellungiella*: role of the plastid terminal oxidase as an alternative electron sink. *Plant Physiology* 149: 1154–1165.
- Takemura T, Hanagata N, Sugihara K, Baba S, Karube I, Dubinsky Z. 2000. Physiological and biochemical responses to salt stress in the mangrove, *Bruguiera gymnorhiza*. *Aquatic Botany* 68: 15–28.
- Tattini M, Lombardini L, Gucci R. 1997. The effect of NaCl stress and relief on gas exchange properties of two olive cultivars differing in tolerance to salinity. *Plant and Soil* 197: 87–93.
- Thomas D, Middleton N. 1993. Salinization: new perspectives on a major desertification issue. *Journal of Arid Environments* 24: 95–105.
- Tognetti R, D'Andria R, Sacchi R, Lavini A, Morelli G, Alvino A. 2007. Deficit irrigation affects seasonal changes in leaf physiology and oil quality of *Olea europaea* (cultivars Frantoio and Leccino). *Annals of Applied Biology* 150: 169–186.
- Turner N, Jones M. 1980. Turgor maintenance by osmotic adjustment: a review and evaluation. In: Turner NC, Kramer PJ, eds. *Adaptation of plants to water and high temperature stress*. New York, NY, USA: Wiley Interscience, 87–103.
- Tyerman SD, Munns R, Fricke W, Arsova B, Barkla BJ, Bose J, Bramley H, Byrt C, Chen Z, Colmer TD *et al.* 2019. Energy costs of salinity tolerance in crop plants. *New Phytologist* 221: 25–29.
- Tyree MT, Sperry JS. 1989. Vulnerability of xylem to cavitation and embolism. *Annual Review of Plant Physiology* 40: 19–36.
- Urli M, Porté AJ, Cochard H, Guégant Y, Burelt R, Delzon S. 2013. Xylem embolism threshold for catastrophic hydraulic failure in angiosperm trees. *Tree Physiology* 33: 672–683.
- Venturas MD, Sperry JS, Hacke UG. 2017. Plant xylem hydraulics: what we understand, current research, and future challenges. *Journal of Integrative Plant Biology* 59: 356–389.
- Venturas MD, Sperry JS, Love DM, Frehner EH, Allred MG, Wang Y, Anderegg WR. 2018. A stomatal control model based on optimization of carbon gain versus hydraulic risk predicts aspen sapling responses to drought. *New Phytologist* 220: 836–850.

- Vico G, Manzoni S, Palmroth S, Weih M, Katul GG. 2013. A perspective on optimal leaf stomatal conductance under CO<sub>2</sub> and light co-limitations. *Agricultural & Forest Meteorology* 182: 191–199.
- Volpe V, Manzoni S, Marani M, Katul GG. 2011. Leaf conductance and carbon gain under salt-stressed conditions. *Journal of Geophysical Research: Biogeosciences* 116: G04035.
- Wang Y, Nii N. 2000. Changes in chlorophyll, ribulose biphosphate carboxylase-oxygenase, glycine betaine content, photosynthesis and transpiration in *Amaranthus tricolor* leaves during salt stress. *Journal of Horticultural Science and Biotechnology* 75: 623–627.
- Wendelberger KS, Richards JH. 2017. Halophytes can salinize soil when competing with glycophytes, intensifying effects of sea level rise in coastal communities. *Oecologia* 184: 729–737.
- Wicke B, Smeets E, Dornburg V, Vashev B, Gaiser T, Turkenburg W, Faaij A. 2011. The global technical and economic potential of bioenergy from salt-affected soils. *Energy & Environmental Science* 4: 2669–2681.
- Williams M, Rastetter EB, Fernandes DN, Goulden ML, Wofsy SC, Shaver GR, Melillo JM, Munger JW, Fan SM, Nadelhoffer KJ. 1996. Modelling the soil-plant-atmosphere continuum in a *Quercus-Acer* stand at Harvard forest: the regulation of stomatal conductance by light, nitrogen and soil/plant hydraulic properties. *Plant, Cell & Environment* 19: 911–927.
- Wolf A, Anderegg WRL, Pacala SW. 2016. Optimal stomatal behavior with competition for water and risk of hydraulic impairment. *Proceedings of the National Academy of Sciences, USA* 113: E7222–E7230.
- Woodward FI, Bazzaz FA. 1988. The responses of stomatal density to CO<sub>2</sub> partial pressure. *Journal of Experimental Botany* 39: 1771–1781.
- Xu C, Tang X, Shao H, Wang H. 2016. Salinity tolerance mechanism of economic halophytes from physiological to molecular hierarchy for improving food quality. *Current Genomics* 17: 207–214.
- Yarami N, Sepaskhah AR. 2015. Physiological growth and gas exchange response of saffron (*Crocus sativus* L.) to irrigation water salinity, manure application and planting method. *Agricultural Water Management* 154: 43–51.
- Yensen NP, Biel KY. 2006. Soil remediation via salt-conduction and the hypotheses of halosynthesis and photoprotection. In: Khan MA, Weber DJ, eds. *Ecophysiology of high salinity tolerant plants*. Berlin, Germany: Springer, 313–342.
- Yeo AR, Caporn SJM, Flowers TJ. 1985. The effect of salinity upon photosynthesis in rice (*Oryza sativa* L.): gas exchange by individual leaves in relation to their salt content. *Journal of Experimental Botany* 36: 1240–1248.
- Yeo AR, Lee AS, Izard P, Boursier PJ, Flowers TJ. 1991. Short- and long-term effects of salinity on leaf growth in rice (*Oryza sativa* L.). *Journal of Experimental Botany* 42: 881–889.
- Zarco-Tejada PJ, Miller JR, Morales A, Berjón A, Agüera J. 2004. Hyperspectral indices and model simulation for chlorophyll estimation in open-canopy tree crops. *Remote Sensing Applications: Society and Environment* 90: 463–476.
- Zhou M, Butterbach-Bahl K, Vereecken H, Brüggemann N. 2017. A meta-analysis of soil salinization effects on nitrogen pools, cycles and fluxes in coastal ecosystems. *Global Change Biology* 23: 1338–1352.
- Zimmermann U, Zhu JJ, Meinzer FC, Goldstein G, Schneider H, Zimmermann G, Benkert R, Thürmer F, Melcher P, Webb D *et al.* 1994. High molecular weight organic compounds in the xylem sap of mangroves: Implications for long-distance water transport. *Botanica Acta* 107: 218–229.

## Supporting Information

Additional Supporting Information may be found online in the Supporting Information section at the end of the article.

**Dataset S1** Literature data used in the main text meta-analysis (Fig. 2a; Table S1), and in the comparison between modeled and observed relative transpiration rate as a function of salinity (Fig. 4c–f; Table S2).

**Fig. S1** Comparison of modeled and measured assimilation rate  $f_c$  as a function of stomatal conductance to water vapor  $g_s$  in *R. mangle* (salt-tolerant) and *O. europea* (salt-sensitive).

**Notes S1** Assumptions required to model root-level salt exclusion.

**Notes S2** Conventions and units adopted to define water fluxes.

Please note: Wiley Blackwell are not responsible for the content or functionality of any Supporting Information supplied by the authors. Any queries (other than missing material) should be directed to the *New Phytologist* Central Office.



## About New Phytologist

- *New Phytologist* is an electronic (online-only) journal owned by the New Phytologist Trust, a **not-for-profit organization** dedicated to the promotion of plant science, facilitating projects from symposia to free access for our Tansley reviews and Tansley insights.
- Regular papers, Letters, Research reviews, Rapid reports and both Modelling/Theory and Methods papers are encouraged. We are committed to rapid processing, from online submission through to publication 'as ready' via *Early View* – our average time to decision is <26 days. There are **no page or colour charges** and a PDF version will be provided for each article.
- The journal is available online at Wiley Online Library. Visit **www.newphytologist.com** to search the articles and register for table of contents email alerts.
- If you have any questions, do get in touch with Central Office (np-centraloffice@lancaster.ac.uk) or, if it is more convenient, our USA Office (np-usaoffice@lancaster.ac.uk)
- For submission instructions, subscription and all the latest information visit **www.newphytologist.com**